FINAL REPORT

Spatially-explicit impacts of climate on past, present, and future fire regimes in Alaskan boreal forest and tundra ecosystems

JFSP PROJECT ID: 14-3-01-07

June 2017

Dr. Luigi Boschetti (PI)
College of Natural Resources, Univ. of Idaho

Dr. Philip E. Higuera (Co-PI)*
Dept. Ecosystem and Conservation Sciences, Univ. of Montana
*Original PI prior to moving institutions; point of contact for project inquires.

Student Investigator: Adam M. Young
Dept. Forest, Rangeland, and Fire Sciences, Univ. of Idaho

FIRESCIENCE.GOV
Research Supporting Sound Decisions






Table of Contents

List of Tables

List of Figures

List of Abbreviations/Acronyms

FF – Fire Frequency

FRP – Fire Rotation Period

MFI – Mean Fire Return Interval

GCM – Global Climate Model

RCP – Representative Concentration Pathway

Keywords

Alaska, boreal forests, climate change, fire regime, fire-climate relationships, paleoecology, statistical modeling, thresholds, transferability, tundra.

Acknowledgements

We thank J. Abatzoglou, P. Duffy, and F. S. Hu for help improving the analysis, interpretation, and text for peer-reviewed manuscripts related this research. We also thank M. Leonawicz for helpful comments and support in downscaling the climate data used in this project. Additionally, we thank the University of Idaho and University of Montana for institutional support, and the Alaskan Fire Science Consortium for providing resources to give a webinar presentation.

Abstract

Projections of future fire activity from statistical models are a powerful tool for anticipating 21st-century fire regimes. In previous work, we developed a set of statistical models that predict the likelihood of fires over 30-yr timescales in Alaskan boreal forest and tundra ecosystems. These models reveal that fire-climate relationships are strongly nonlinear, exhibiting distinct climatic thresholds to burning. Driving these models with future climate projections further highlights the potential for fire-regime shifts to occur as climatic thresholds are crossed as climate warms, with some tundra and forest-tundra regions projected to experience at least a fourfold increase in the probability of burning. These projections are also accompanied by significant sources of uncertainty, particularly related to the calibration of statistical models using data spanning the relatively short observational period (i.e., 1950-2009). The goal of this project was to evaluate the ability of our statistical models to predict outside the observational record, and thus identify key strengths and limitations when applying statistical models to predict fire activity under scenarios of 21st-century climate change.

We compared statistical predictions with independent fire-history reconstructions spanning the late Holocene (i.e., 850-1850 common era [CE]), developed from sediment charcoal in lake-sediment records. Our statistical models were informed with downscaled Global Climate Model (GCM) data for 850-1850 CE, and predictions were compared to mean fire return intervals estimated for each of 29 published fire-history reconstructions spanning seven Alaskan ecoregions. Our model-paleodata comparisons for 850-1850 CE highlighted varying levels of prediction accuracy among Alaskan ecoregions, with variability strongly related to ecoregion proximity to a summer temperature threshold to burning: regions closer to this threshold exhibited significantly larger prediction errors. In conjunction with this spatially varying prediction accuracy, modifying a modern (i.e., 1950-2009) fire-climate relationship even slightly, resulted in significant changes in prediction accuracy over 850-1850 CE, suggesting future projections would be sensitive to uncertainties in GCMs and/or changes in fire-climate relationships. The sensitivity in future predictions to the presence of a threshold to burning implies that uncertainty will likely shift spatially across Alaska and temporally throughout the 21st century, as different regions approach and surpass climatic thresholds over the course of the century.

Our findings provide key information for understanding how fire regimes may respond to climate change in Alaska, valuable to land and fire managers for anticipating and preparing for future ecosystem change. Specifically, we provide spatially explicit projections of potential future fire regimes, based on the climate suitability to burning. These projections highlight which regions are most vulnerable to climatically induced fire-regime shifts. Additionally, we link these projections with our current understanding of spatial and temporal patterns in threshold-driven uncertainty, highlighting regions where our models are most likely to have high uncertainty. By evaluating both spatial patterns in vulnerability and threshold-driven uncertainty, our results allow managers and policymakers to identify and prioritize resources in preparing for future landscape change.

Objectives

This research was proposed under a Graduate Research and Innovation Award task statement (FON 14-3 Task 01), specifically focusing on the topic of "climate change and fire." The primary aim of this research was to evaluate our ability to statistically model fire regime responses to climate change in Alaskan boreal forests and tundra ecosystems, a priority for Alaskan fire and land managers. To meet this goal, we designed an analysis to evaluate how well observed fire-climate relationships (i.e., from 1950-2009) could predict fire activity in time periods and climatic conditions outside of the observational record, using the late Holocene (850-1850 CE) as an example. Our original objectives were the following:

Objective 1: Drive and validate existing spatially-explicit, multi-decadal models with paleoclimate and paleofire datasets to test their ability to predict mean fire return intervals (*MFI*) under varying climatic conditions. Through this process the models will be iteratively calibrated to maximize their ability to predict the presence or absence of fire throughout the paleo record.

Objective 2: Use the calibrated models to spatially project *MFI* under a suite of IPCC AR5 emissions scenarios and global climate models (GCMs) throughout the 21st-century, and compare these projections with paleofire data to understand precedence of future fire regimes.

Broadly, we were able to achieve both of these objectives. For Objective 1, we were able to successfully drive a set of multidecadal statistical models from Young *et al.* (2017) with downscaled-GCM climate data for the late Holocene (i.e., 850-1850 CE). Model predictions for 850-1850 CE were then compared to paleofire reconstructions from this time period. However, we were not able to iteratively calibrate these statistical models in an effort to constrain future projections of fire activity. We attempted this calibration, but found the GCM data unsuitable for this task, primarily due to cooler-than-likely temperature biases occurring in the GCMs. Therefore, we focused on exploring and understanding patterns in prediction skill among Alaskan ecoregions for 850-1850 CE.

For Objective 2, we were able to provide spatially explicit projections of fire regimes for the 21st century across Alaskan boreal forest and tundra ecosystems, published in Young *et al.* (2017). These future projections are currently described in Young *et al.* (2017) as well as in this final report.

While this research focuses on Alaska, our results further revealed key uncertainties accompanying predictions of ecosystem properties governed by threshold relationships in general. Given the prevalence of threshold relationships in ecological systems, and their fundamental importance for understanding ecological concepts such as resilience and alternative stable states (Gunderson 2000), our findings have implications beyond the challenge of understanding future fire activity in Alaska. Thus, we chose to further investigate and understand these threshold-caused patterns in prediction uncertainty, and we include this as a significant component of this JFSP-funded research. In this report, we present these results in this broader context, while also relaying key findings and implications specific to Alaskan fire regimes.

Background

Anticipating how 21st-century climatic and environmental changes may alter ecosystem structure and function is a key challenge for ecologists, with implications for biogeochemical cycling, natural resources management, and human livelihoods (Walther *et al.* 2002; Grimm *et al.* 2013). Statistical models are a key tool for anticipating potential ecosystem impacts (Guisan & Zimmermann 2000; Elith & Leathwick 2009; Krawchuk & Moritz 2014), projecting future changes based on observational relationships among ecological and climatic variables. When driven with projections from GCMs, statistical models provide a valuable depiction of potential 21st-century change and ecosystem states (Elith & Leathwick 2009). For example, under anthropogenic climate change, fire activity is projected to shift significantly, at regional (e.g., Balshi *et al.* 2009; Hu *et al.* 2015; Young *et al.* 2017) to global (e.g., Krawchuk & Moritz 2009; Moritz *et al.* 2012) scales. Statistical projections, however, are also accompanied by important limitations and uncertainties. One key limitation is the assumption that statistical models are transferable in time and space, and thus able to accurately predict beyond the observational record (Thomas & Bovee 1993; Wenger & Olden 2012). The term used to describe this ability is "transferability." Evaluating transferability, and thus the ability of statistical relationships to predict and track climate-induced ecological change, is critical for understanding uncertainties accompanying projections of future ecosystem change.

Multiple studies have highlighted variability in predictions outside the observational record, whether in new time periods in the past or future (Diniz-Filho *et al.* 2009; Moreno-Amat *et al.* 2015), or in new regions in space (Randin *et al.* 2006; Aertsen *et al.* 2010). This variability can be traced to one of two general sources of prediction uncertainty: model specification or data inaccuracies (Barry & Elith 2006). Uncertainty due to model specification can be related to differences among modeling tools (i.e., flexibility, optimization, and extrapolation), the inclusion or exclusion of different explanatory variables, or non-stationary (i.e., changing) ecological relationships across space or time; correspondingly, data inaccuracies can lead to uncertainty by introducing biased depictions of reality (Regan *et al.* 2002; Heikkinen *et al.* 2006). This sensitivity of statistical predictions to model specificity and/or data inaccuracies may also be linked to and interact with inherent complexities common in ecological relationships, and in particular, the presence of threshold responses (Peters *et al.* 2004a).

Wildfire is a classic example of a process that is strongly controlled by threshold relationships (e.g., Peters *et al.* 2004b; Flannigan & Harrington 1988; Pausas & Paula 2012; Young *et al.* 2017), and thus future predictions wildfire activity (e.g., probability of occurrence, severity) are subject to the influences of these threshold relationships. In general, our ability to predict changes in threshold-governed ecosystem properties may be limited due to the wide range of values a property can have over a relatively small range of an ecosystem driver. For example, we may find that a relationship between the mean fire return interval (*MFI* [yr]) and a climatic control is distinctly nonlinear and exhibits a threshold response (Figure 1a). In this example, as climate conditions cross this threshold, *MFI* would change from >3000 yr below the threshold to < 200 yr above the threshold, exhibiting heightened fire-regime variability over a small change in climate. In contrast, in a system with a more linear fire-climate relationship, changes are more gradual and exhibit less variability for a similar change in climate (Figure 1b, c). Under heightened ecosystem variability inherent in a threshold relationships (e.g., Figure 1a),

prediction uncertainty will also likely be higher, as predictions will be sensitive to either variability in model specification (e.g., non-stationary or changing fire-climate relationships), or to inaccuracies in the data used to calibrate and drive the models.

The impact of the presence of threshold relationships may also lead to locally varying levels of threshold-driven uncertainty across space and time (e.g., Elith *et al.* 2002; Wenger *et al.* 2013). Under threshold responses, as climate continues to change, different geographic regions will approach and surpass climatic thresholds at different time periods. In the context of fire regimes, this means that predicting the timing and location of a fire-regime shift may be inherently more difficult and less accurate, as certain regions will inherently lie closer to a threshold value and thus be more sensitive to potential data inaccuracies and/or varying relationships when predicting future change. Characterizing locally varying levels of uncertainty in predicted fire activity is critical to consider in the context of fire management and anticipating future fire-regime shifts. For example, if similar levels of fire-regime change are predicted in two different regions, but uncertainty in one region is significantly higher, land managers may utilize available resources differently when monitoring and preparing for oncoming regime shifts.

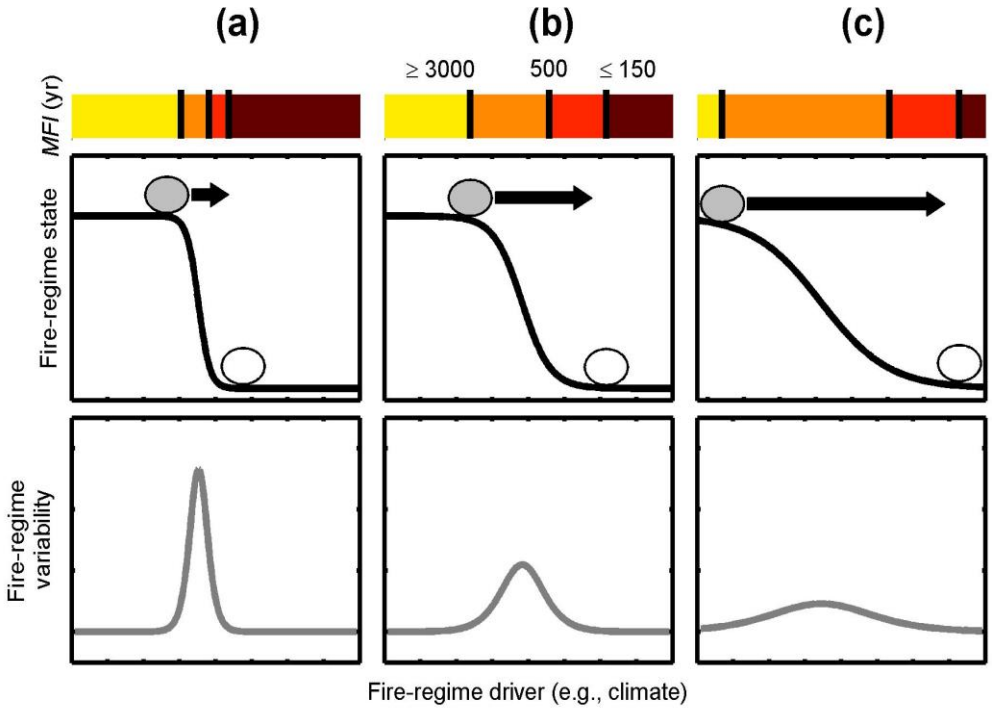

Figure 1. Conceptual framework of how differing fire-climate relationships may impact statistical predictions. In the leftmost column (a), a distinct threshold highlights that a significant fire-regime change can occur over a relatively small change in climate (length of arrow). Under more linear relationships (b-c), a larger change in climate is needed to drive the same fire-regime shift. Accompanying these different relationships, are different levels of fire-regime variability in response to climate (specifically measured in terms of mean fire return intervals; *MFI*). For example, in (a) there is high variability immediately surrounding the distinct threshold, and any data inaccuracies or model misspecification may lead to higher probability of committing significant prediction error.

To evaluate how the presence of threshold relationships may impacts our ability to predict future fire-regime change, and how this threshold-driven uncertainty may unfold across space and time, we designed an analysis to evaluate how well statistical predictions compare with independent observations outside the observational record (Graham *et al.* 2004; Martínez-Meyer *et al.* 2004). Specifically, we compare statistical predictions with paleofire reconstructions during the late Holocene (850-1850 CE). Paleoecologial reconstructions are a valuable resource for evaluating predictions outside the observational record, as they offer estimates of past ecological activity that span hundreds to thousands of years (Jacobson 1988). Additionally, Alaska is ideal for this analysis, due to the extensive knowledge of fire-climate relationships (Duffy *et al.* 2005; Hu *et al.* 2015; Young *et al.* 2017) and the availability of fire-history datasets spanning at least the past 1200 years (Higuera *et al.* 2009; Hu *et al.* 2010; Higuera *et al.* 2011a; Barrett *et al.* 2013; Kelly *et al.* 2013; Chipman *et al.* 2015).

Materials and methods

Study area

Our study area is mainland Alaska (Figure 2), dominated by boreal forest and tundra ecosystems. Boreal forests generally experience moderate- to high-severity fire events, with mean fire return intervals ranging from 120-250 yr (Kasischke *et al.* 2002). In the Noatak River Watershed (Figure 2), the most flammable region of Alaskan tundra, mean fire return intervals over the past two millennia have been comparable to those in interior boreal forest (Higuera *et al.* 2011). In cooler tundra ecoregions, such as the Brooks Foothills and Yukon-Kuskokwim Delta, mean fire return intervals exceed (sometimes greatly) 3500 yr (Hu *et al.* 2010; Chipman *et al.* 2015). A detailed description of the vegetation communities in these Alaskan ecosystem is described in Young *et al.* (2017).

Statistical models of fire presence/absence

To understand the impacts of predicting fire activity beyond the observational record, we tested the ability of a set of statistical models predicting fire activity in Alaska (Young *et al.* 2017) to predict fire activity over the past millennium (850-1850 CE). These models were designed to predict the spatially explicit 30-yr probability of fire occurrence at 2-km resolution in Alaskan boreal forest and tundra ecosystems. This group of models is classified as "AK" in Young *et al.* (2017). Models were constructed by relating the spatial distribution of fire presence/absence to climatological normals of average temperature of the warmest month (i.e., summer temperature, T_{WARM}, °C) and total annual moisture availability (i.e., precipitation minus potential evapotranspiration, P-PET, mm), as wells as topographic ruggedness and land-cover type. The relationships among fire, climate, topography, and vegetation were quantified using Boosted Regression Tree models (BRTs), a machine learning tool (Friedman 2001, 2002). Young *et al*. (2017) provide a set of 100 individual BRTs, with each BRT unique due to internal model-building stochasticity and a random selection of observations from the study area. A key finding from Young *et al.* (2017) was the importance of summer temperature as an explanatory variable for fire presence/absence, and a distinct threshold response between summer temperature and the 30-yr probability of fire occurrence. The estimated mean (bootstrapped 95% CI) threshold value for T_{WARM} was 13.40 °C (13.29, 13.45), calculated using a segmented

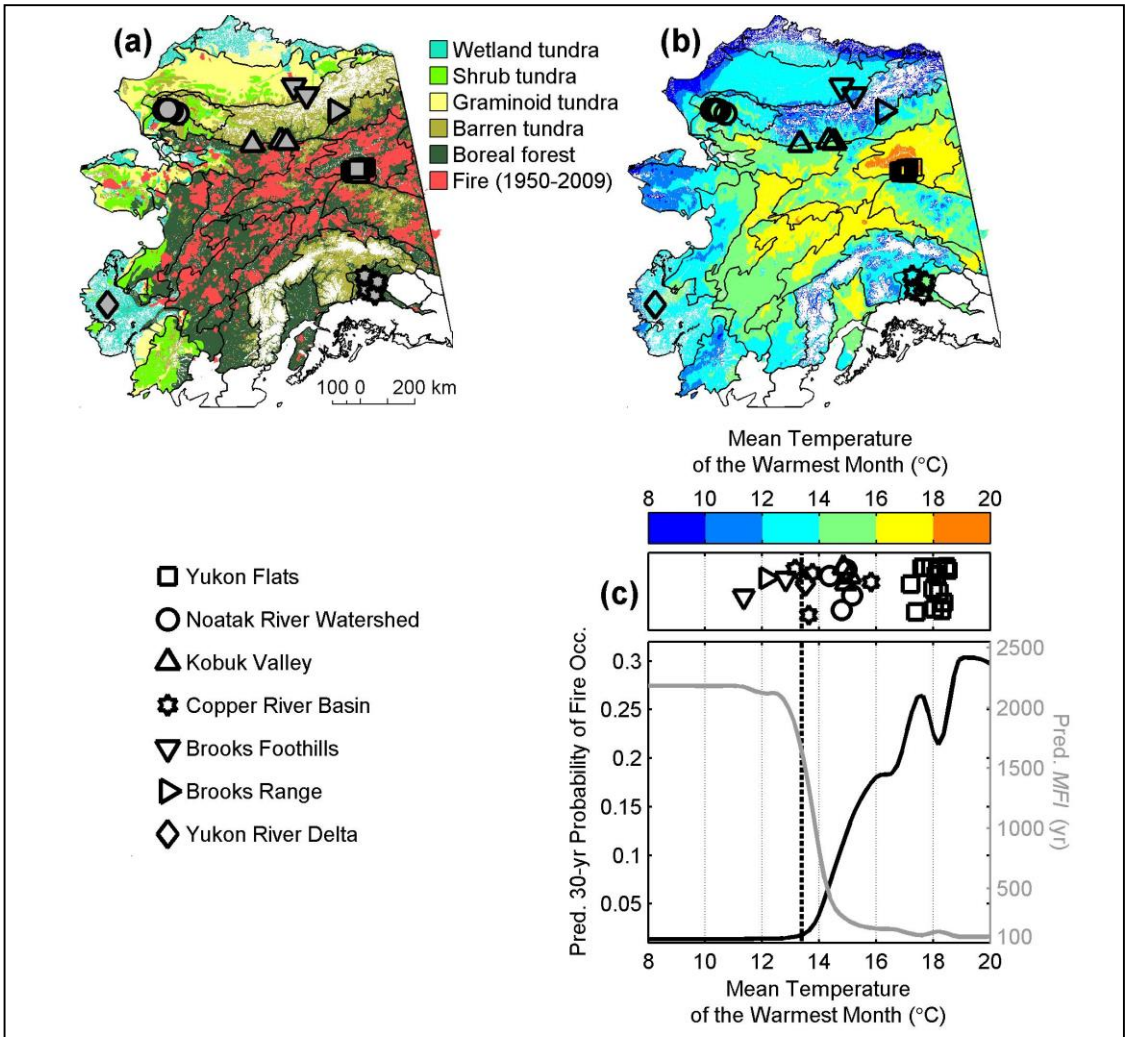

Figure 2. Alaskan study area, including vegetation, fire history from 1950-2009, climate, and a key modeled fire-climate relationship. (a) Spatial distribution of modern vegetation and recent fire occurrence (1950-2009) at 2-km resolution. Plotted symbols represent locations of individual fire-history reconstructions, and different symbols represent different ecoregions. (b) Mean temperature of the warmest month (°C) from 1950-2009, the most important control of fire occurrence in Alaska during the observational record (Young *et al.* 2017). (c) Modeled observational relationships between the probability of fire occurrence and mean temperature of the warmest month at a 30-yr timescale. The vertical line at 13.4 °C is the threshold value estimated in Young *et al.* (2017). The upper panel in (c) displays the distribution of lake locations in univariate climate space along T_{WARM}. The plotting of lake locations includes a vertical "jittering" to reduce overlapping of symbols. For reference, the gray line is the inverse of the black line, an approximation of the mean fire return interval (*MFI*), and is displayed due to the use of this metric to evaluate model-paleodata comparisons. Polygons in (a-b) indicate individual ecoregions classified at Level III, and are slightly modified from those in Nowacki *et al.* (2001).

regression analysis (Muggeo 2003). We used the published models from Young *et al*. (2017) for this study, with one notable modification. Here, we use mean total annual precipitation (mm) instead of annual moisture availability (i.e., P-PET), because estimates of potential

evapotranspiration (PET) are subject to more sources of uncertainty relative to estimates of precipitation, due to the number of different methods used to calculate PET (McAfee 2013). Thus, we chose variables provided directly by global climate model (GCM) simulations (i.e., precipitation), as opposed to incorporating additional calculations and potential uncertainty accompanying the use of PET. Results of these updated models were comparable to those from Young *et al.* (2017).

Past-millennium climate data

To predict fire activity over the past millennium, we informed the statistical models with bias-corrected and spatially downscaled paleoclimate data spanning 850-1850 CE, a time period outside the observational record (i.e., 1950-2009 CE). Specifically, we used GCM simulations from the Paleoclimate Intercomparison Project Phase 3 (PMIP3, Braconnot *et al.* 2012), a component of the Coupled Model Intercomparison Project (CMIP5, Taylor *et al*. 2012). We used GCMs instead of paleoclimate reconstructions because most paleoclimate reconstructions in Alaska are not spatially collocated with the paleoecological fire-history records used for validation (see *Model- paleofire comparisons*). We initially collected available GCMs from the PMIP3 experiments that met the following criteria: (1) were at a monthly timescale from 850-1850 CE and (2) provided atmospheric output for surface air temperature and precipitation. Five GCMs from the Earth System Grid Federation repository (https://www.earthsystemcog.org/projects/cog/) met these requirements (as of March 1, 2017): GISS-E2-R, IPSL-CM5A-LR, MPI-ESM-P, MIROC-ESM, and MRI-CGCM3. A ranking analysis, similar to that used by Rupp *et al.* (2013), was used to evaluate the relative performance of each GCM from 1950-2000 in mainland Alaska. Based on this ranking analysis, we used the top three GCMs to drive our statistical models over the past millennium: GISS-E2-R, MPI-ESM-P, and MRI-CGCM3. We used each GCM individually to drive our statistical models and calculate prediction error (see *Model-paleofire comparison*). To account for differences in the spatial resolution between our statistical models (2 km) and GCMs (i.e., > 1.0° latitude × longitude), we conducted a bias correction and downscaling analysis using the delta-change method (Giorgi & Mearns 1991). The full details on the ranking and downscaling analyses are described in appendices D and E, respectively.

Model-paleofire comparisons

We used published paleofire records as an independent data source to validate our statistical models when applied outside the observational record. Specifically, we compared model predictions to fire-history reconstructions derived from 29 lake-sediment charcoal records that span seven ecoregions in Alaska (Figure 2). In each record, local fire events were estimated using a statistical technique that identifies significant peaks in charcoal accumulation rates (CHAR) relative to background CHAR (Higuera *et al.* 2009), with "local" defined as a radius of approximately 500-1000 meters around each lake. Thus, the approximate spatial scale represented by each lake-sediment record (0.8-3.1 km^2) is reasonably well matched to the 2-km pixel resolution (i.e., 4 km^2) used in the statistical models. Details and metadata for each of these records are presented in Appendix F. Using these charcoal peaks, fire frequency and mean fire return intervals (Eqn. 1) were calculated for each lake location over a given time period. Since the statistical models used here quantify the 30-yr probability of fire occurrence for a specific 4-

km^2 pixel on the landscape, these predictions can be equated to the annual probability of any given pixel burning, and thus further equated to fire frequency through the cumulative summation of the predicted annual probability of fire occurrence (Johnson & Gutsell 1994). In this analysis, we specifically used the inverse of fire frequency (*FF*) to compare predictions and observations, $FF^{-1} = t/N_{FIRES}$. Here, *t* is the number of years during the time period of prediction or reconstruction (in this analysis 1000 yr [850-1850 CE]), and N_{FIRES} is equal to the number of fire events predicted or reconstructed during this 1000-yr period. We used the inverse *FF* to compare predictions and observations, as under large-samples the inverse *FF* can approximate the mean fire return interval (*MFI* [yr]), a more commonly used metric to interpret fire frequency across different landscapes (i.e., $FF^{-1} = t/N_{FIRES} \approx MFI$).

We measured prediction error to evaluate differences between model predictions and reconstructed *MFI* and understand the relative accuracy of our model predictions. Specifically, we used a standardized prediction-error metric (Eqn. 1).

$$E_{i,j,k} = \frac{P_{i,j,k} - O_{i,j}}{\overline{O}_{\bullet,j}} \times 100 \quad (1)$$

Here, $E_{i,j,k}$ is the standardized error metric for the k^{th} BRT ($k = 1, 2, \ldots, 100$), j^{th} ecoregion ($j = 1, 2, \ldots, 7$), and i^{th} lake-sediment record ($i = 1, 2, \ldots, n_j$), where n_j is the number of lakes in the j^{th} ecoregion. *P* is the model prediction, *O* is the observed *MFI* for the time period of 850-1850 CE, and $\overline{O}$ in the denominator (Eqn. 1) is the average *MFI* from all lakes within each ecoregion (i.e., $n_j^{-1} \sum_{i=1}^{n_j} MFI_i$). Standardizing this error metric by the average *MFI* accounts for differing levels of fire frequency among ecoregions. A tradeoff with this standardization is the possibility for ecoregions to have no fires from 850-1850 CE, resulting in a denominator value equal to infinity (i.e., 1000 yr / 0 fires). To account for this outcome, if a lake had no fires within the past millennium, we calculated $\overline{O}$ based on an extended time period that captured the most recent fire event in the paleo-fire-history record. Among all lakes, this extended time period was never earlier than 5019 BCE (i.e., Before Common Era; Appendix F).

Sensitivity analysis

To evaluate the sensitivity of model predictions to potential sources of uncertainty, we modified observational fire-climate relationships in Alaska, comparing predictions between modified and unmodified relationships. When modifying these relationships, we only altered the marginal relationship between T_{WARM} and the probability of fire occurrence. This was justified based on results from Young *et al*. (2017), which indicate that T_{WARM} is the most important variable explaining fire occurrence. We modified two specific aspects of observational relationships: (1) the shape of the relationship, and (2) the location of the T_{WARM} threshold. These two modifications were designed to evaluate the sensitivity of model predictions to key sources of predictions uncertainty: model specification or data inaccuracies. "Model specification" refers how the shape and nature of a fire-climate relationship is captured by a statistical tool; "data inaccuracies" include biases or inaccuracies occurring in the data used to calibrate or drive statistical models. We modified the relationship between T_{WARM} and the probability of fire by

altering the training dataset; the result is three modified relationship shapes, each increasingly more linear compared to the original (Appendix G). We modified the location of the climatological threshold by adding 0.5 °C, 1.0 °C, and 1.5 °C to the downscaled GCM-based temperature estimates. By modifying the temperature values of T_{WARM} we effectively shifted the climatological location of the threshold, thus testing the sensitivity of model prediction error to potential data inaccuracies.

Projecting 21st-century fire regimes

We compared historical and future projections of the probability of fire occurrence to understand potential fire regimes under projected climate changes. We used downscaled (2 km) 21st-century projections from five general climate models (GCMs) from the Coupled Model Intercomparison Project Phase 5, provided by the Scenarios Network for Alaska and Arctic Planning (2015), under the Representative Concentration Pathway 6.0 scenario (CCSM4, GFDL-CM3, GISS-E2-R, IPSL-CM5A-LR, and MRI-CGCM3). These specific models were selected because they were evaluated as most skillful for Alaska, based on a ranking analysis performed by Walsh *et al.* (2008). Unfortunately, not all GCMs provide projections for the past millennium, and so this set of five GCMs differs from those used for our retrospective predictions. We used the large set of five GCMs for future projections, here and as published by Young et al. (2017), because we deemed this larger ensemble more robust and more appropriate for making future projections. We informed our models with 30-yr averages of T_{WARM} and $P\text{-}PET_{ANN}$ (i.e., total annual moisture availability [mm]; see *Statistical models of fire presence/absence*) for 2010-2039, 2040-2069, 2070-2099 for each 2-km pixel under each GCM. Our BRTs were then driven with 30-yr climatological normals, while keeping our topographic and vegetation variables unchanged.

To quantify fire-regime responses to future climate change projections we calculated the fire rotation period for each 2-km pixel. To quantify the direction and magnitude of potential fire-regime changes, we present a ratio between projected future fire rotation periods (FRP_{Future}) and historical fire rotation periods ($FRP_{Historical}$), for each pixel (i.e., FRP_{Future} / $FRP_{Historical}$) (e.g., Boulanger et al. 2013). This ratio is < 1.0 if fire activity increases and projected fire rotation periods shorten, and > 1.0 if fire activity decreases and projected fire rotation period lengthen. For both projected FRP and the relative change in FRP, we displayed the median predicted value from all 5 GCMs, as well as projections from the warmest (GFDL-CM3) and the coldest GCMs (MRI-CGCM3), defined as T_{WARM} averaged over Alaska from 2010-2099.

Uncertainty in projections of 21st-century fire-regime projections

Initial results from using our statistical models to predict fire activity over the past millennium revealed increased prediction error in regions near the summer temperature threshold, implying spatially varying uncertainty in future projections. To understand the spatial distribution of Alaskan landscapes that lies relatively close the summer temperature threshold, and thus where predictions may be accompanied by threshold-driven uncertainty, we conducted an additional analysis. Specifically, we classified each pixel in Alaska by its proximity to the temperature threshold, as either below (≤ 11.4 °C), near (>11.4 °C and ≤ 15.4 °C), or above (>15.4 °C) the threshold. This classification was done for 2010-2039, 2040-2069, and 2070-2099

for the warmest (GFDL-CM3) and coolest (MRI-CGCM3) GCMs from the five provided by the Scenarios Network for Alaska and Arctic Planning (2015), as well as the median of these five GCMs (in terms of projected warming, IPSL-CM5A-LR). This was done for the RCP 6.0 scenario.

Results and discussion

Dissemination of research results

The findings we present here have been featured and disseminated through multiple presentations at professional conferences, guest lectures in undergraduate fire ecology courses at the University of Montana, a webinar presentation to the Alaska Fire Science Consortium (part of the JFSP Fire Science Exchange Network; https://www.frames.gov/partner-sites/afsc/home/), and peer-reviewed publication in the journal *Ecography* (Impact Factor = 4.902). In addition to these completed deliverables, we are also planning to submit another manuscript for publication. This second publication will focus on the implications of predicting ecological change in systems characterized by threshold relationships. Finally, the published work in Young *et al.* (2017) and the manuscript in preparation will each be featured as separate chapters in student investigator Young's dissertation. A full list of these completed and planned deliverables is given in Appendix B.

Predicting fire activity outside the observational record

Our findings highlight varying levels of prediction error among Alaskan ecoregions for 850-1850 CE, with higher prediction errors in regions closer (in climate space) to an observed summer temperature threshold to burning of 13.4 °C, and relatively low in regions further away from this temperature threshold (Figure 3). For example, in the Yukon Flats (on average 4.6 °C [SD = 0.4 °C] above the T_{WARM} threshold), the median prediction error among all lakes, GCMs, and BRTs (i.e., 14 lakes × 3 GCMs × 100 BRTs) was -20%, with an interquartile range (IQR) of 63% (IQR = third minus first quartile). Therefore, since *MFI* is being used in these comparisons, in the Yukon Flats our models slightly over predicted burning relative to paleo-fire records. In contrast, in regions sitting closer to the identified threshold, such as the Copper River Basin (0.7 °C above the threshold [SD = 1.2 °C]) and the Noatak River Watershed (1.4 °C above the threshold [SD = 0.3 °C]), median prediction errors were 491% (IQR = 472%) and 153% (IQR = 444%), respectively (Figure 3). The exception

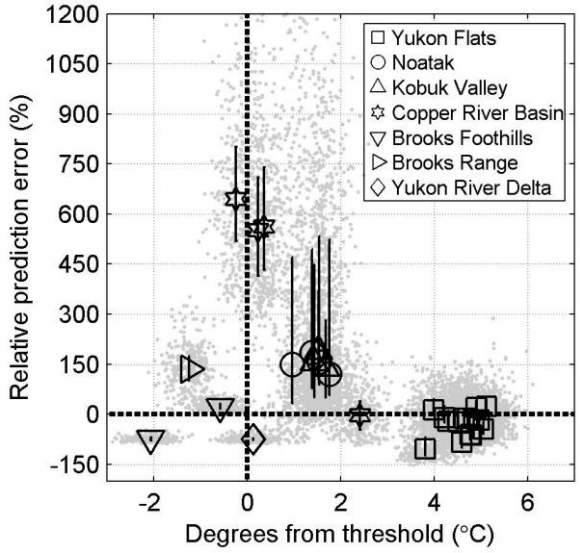

Figure 3. Relative prediction errors for each lake in the study area during 850-1850 CE. Dark-colored symbols represent the median prediction error for all 300 predictions for each lake (i.e., all BRTs [n = 100] and GCMs [n = 3]). Confidence bounds represent the 25th to 75th percentiles of prediction errors. Gray dots are prediction errors associated with an individual BRT, GCM, and paleo-record.

to this pattern occurred in tundra regions that experienced little fire activity over the past millennium. For example, the prediction error in the Yukon-Kuskokwim Delta, which today sits relatively close to the 13.4 °C threshold (0.13 °C above), had a median prediction error of only -76% on average (IQR = 9%; Figure 3).

This increased prediction error in regions near the temperature threshold may be related to heightened variability of ecosystem states, in both time and space (e.g., Figure 1). Increased ecosystem variability is commonly used as a metric for monitoring and anticipating impending regime shifts (Biggs *et al.* 2009; Scheffer *et al.* 2009; Kefi *et al.* 2013). However, in the context of statistical prediction (as opposed to ecosystem monitoring over time), increased ecosystem variability near thresholds inherently decreases predictability, as slight changes in an ecosystem driver are related to sudden changes in ecosystem states (Peters *et al.* 2004; Figure 1), thereby increasing uncertainty for statistical predictions outside the observational record. In the context of Alaskan fire regimes, this variability in the probability of fire near the summer temperature threshold may be linked to increased variability in the frequency of climate conditions conducive for landscape burning, and/or spatial variability in flammable vegetation (Turner & Romme 1994).

Sensitivity of predictions to altered fire-climate relationships

Modifying the value of the summer temperature threshold to burning significantly changed prediction errors in ecoregions closer to the observed temperature threshold, while causing relatively no change in other ecoregions (Figure 4). For example, in the Noatak River Watershed and the Kobuk Valley, decreasing threshold values by only 0.5 °C relative to the original (unmodified) relationship decreased the median prediction error by approximately 98% and 94%, respectively. Conversely, in the Yukon Flats and less-flammable tundra regions (e.g., Brooks Foothills), increasing temperature values, even as much as 1.5 °C, did not significantly alter the prediction errors (Figure 4). This sensitivity of model predictions in our analysis helps highlight how statistical predictions may further be sensitive to data inaccuracies, such as bias in GCM estimates. In our sensitivity analysis, modified threshold values lead to significant variability in prediction error (Figure 4), particularly in regions near the summer temperature threshold. In contrast, prediction error was much lower in regions further away from the summer temperature thresholds (Figure 4). This result further highlights the impact threshold responses can have high on uncertainty in future projections when using different GCMs and/or emissions scenarios. Beyond Alaskan fire regimes, similar uncertainties across space and time are found when statistically predicting species' range shifts, which is at least partly attributable to variability among GCMs and emissions scenarios (Diniz-Filho *et al.* 2009; Wenger *et al.* 2013; Watling *et al.* 2015). Although these patterns of varying uncertainty in species range shifts have not been explicitly linked to threshold responses, a reasonable hypothesis would be that spatial patterns in prediction uncertainty are at least partially related to the influence threshold responses, given that species distributions are governed by complex, nonlinear relationship (Austin *et al.* 1990; Elith & Leathwick 2009).

Statistical predictions were also highly sensitive to changes in fire-climate relationships, highlighting an additional challenge for anticipating future changes in ecosystem properties governed by threshold relationships. In this study, when using any of the three modified

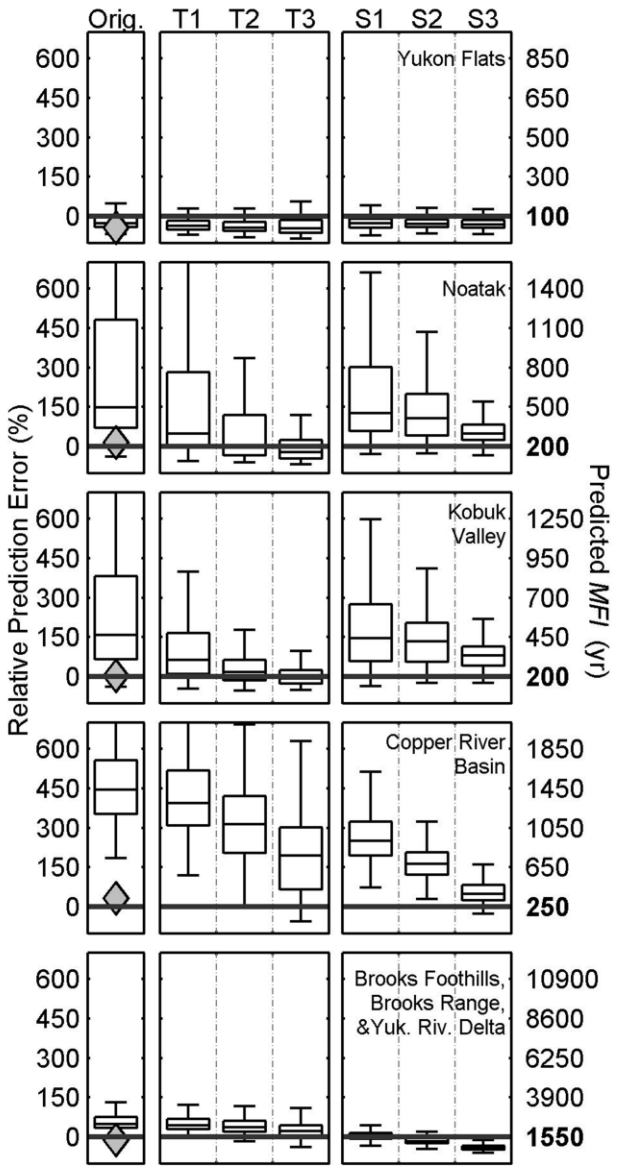

Figure 4. Impacts of modified relationships on prediction error for *MFI* for the 850-1850 CE period, stratified by ecoregion (rows). In the leftmost column, predictions are summarized by using the unmodified, original relationship between temperature and the probability of fire occurrence. For each ecoregion, relative prediction error was averaged across all lakes, and the boxplots display the distribution of this averaged prediction error for all BRTs and GCMs. In the middle column, boxplots display the distribution of prediction errors under three relationships that were modified by shifting the threshold value (T1 = +0.50 °C, T2 = +1.00 °C, and T3 = +1.50 °C). In the rightmost column, boxplots display the distribution of prediction errors under three scenarios where the shape of the relationship was modified (i.e., S1-S3; Appendix G). The right axis represents predicted *MFI*, with the bold value and horizontal line highlighting the observed *MFI* in each ecoregion (rounded to the nearest 50 yr). As a reference, the gray diamond represents the median of the observed relative prediction error for the original 100 BRTs during the historical period (1950-2009).

relationships (Appendix G), the distribution of prediction errors changed considerably in ecoregions near the summer temperature threshold. Specifically, under the two more moderately modified relationships (i.e., S1 & S2), median prediction errors only showed significant decreases in the Copper River Basin (192% and 332% respectively). However, dispersion in prediction errors (measured with the IQR) narrowed considerably, thus indicating a change in the distribution of prediction errors, specifically by 168%, 99%, and 77% under S1, and 253%, 169% and 120% under S2 for the Noatak River Watershed, Kobuk Valley, and Copper River Basin, respectively. Conversely, in the Yukon Flats, the ecoregion furthest away from the observed threshold, the median (IQR) prediction error was stable when using either the original relationship (median = -27%, IQR = 37%), or the three modified relationships (i.e., S1-S3; Appendix G): -27% (34%), and -28% (30%), and -30% (30%) (Figure 4). Therefore, in our

sensitivity analysis, modifications to observational relationships caused notable decreases in prediction error in regions closer to the observed summer temperature threshold (Figure 4). The impact of incremental modifications to observed fire-climate relationships suggests that if relationships change even slightly in the future, then predictions may differ considerably. This sensitivity to modified fire-climate relationships also provides a clear illustration of how model specification can impact prediction uncertainty, particularly in regions that lie near threshold values.

Considering future projections of fire activity, there are several reasons why fire-climate relationships may differ in the past or future, relative to those specified during the observational record. First, differing relationships could be a product of data inaccuracies, such as missing observations (Barry & Elith 2006). In the context of our study, it is well-documented that small fires are likely missing from the Alaska Large Fire Database (Kasischke *et al.* 2002), used to develop the statistical models (Young *et al.* 2017). If these small, missing fires occurred near the observed temperature threshold, this could affect the shape of the modeled relationship between summer temperature and the probability of fire occurrence (e.g., Appendix G). Second, statistical models only depict a "snapshot" of the nature of ecological relationships for a given spatial and temporal scale, and there is likely natural variation in these relationships at finer and/or broader scales (Williams & Abatzoglou 2016). For example, in Canadian boreal forests, fire-climate relationships exhibited important differences between annual and multi-decadal scales (Parisien *et al.* 2014). Finally, changing fire-climate relationships through time may also arise in the past or future through fire-vegetation feedbacks, which mediate the link between climate and fire (Higuera *et al.* 2015).

Projections of future fire regimes

A major goal of this work was to provide projections of future fire activity in Alaska. The average projected climate change among all five GCMs under RCP 6.0 suggests increases in summer temperature (T_{WARM}) across all ecoregions, ranging from 0.73 – 1.19 °C during 2010-2039, to 2.33-3.08 °C by 2070-2099 (Appendix H). Under these projections, the median probability of fire occurrence from among the five GCMs suggests shorter fire rotation periods (i.e., more frequent burning) (Figure 5) in 87%, 93%, and 97% of our study region for 2010-2039, 2040-2069, and 2070-2099, respectively (Figure 6). In 43% of our study area, the probability of burning is projected to more than double by mid-century, resulting in fire rotation periods less than half of that predicted for the historical period. In contrast, 13% of our study region is projected to have no change or reduced fire activity for 2010-2039, primarily in boreal forest regions (Figure 6).

A second major goal of our work was to be able to highlight regions in Alaska that may be most vulnerable to climatically induced changes in fire activity. We found that the largest relative increases in fire activity occur in tundra regions and the cooler boreal forest regions, along the forest-tundra boundary. These large relative increases in tundra and forest-tundra ecosystems were consistent among projections from different GCMs (Figure 6). In ecoregions such as the Brooks Foothills and Yukon-Kuskokwim Delta, fire rotation periods are projected to decrease from greater than 800 to less than 200 years by the end of the 21st century. In boreal forest the relative magnitude of change is smaller than in tundra and forest-tundra regions, but

across most of the boreal forest fire rotation periods are projected either to decrease to less than 100 years by end of the 21st century, or remain relatively unchanged with fire rotation periods ranging from 100-200 yr under the coolest scenario considered (Figure 5). These results therefore highlight spatially varying levels of vulnerability to potential fire-regime shifts across Alaska.

While our models suggest a potential decrease in fire activity in portions of Alaska, either in the early part of the 21st century or under the coolest GCMs, our projections of future fire activity in boreal forest and tundra ecosystems by the end of the 21st century align well with projections of northern-high-latitude fire activity from other studies. For example, Balshi *et al.* (2009) found that annual area burned may increase by up to 200% by the end of the 21st-century warming in boreal forests of North America. Additionally, global analyses depict boreal forest and tundra biomes as particularly susceptible to large increases in the probability of fire occurrence by the end of the 21st century (Moritz *et al.* 2012). In each of these cases, projected increases in fire activity are primarily driven by projected increases in summer temperature and water deficit, as warmer temperatures and drier conditions prime the landscape for broad-scale burning by increasing the fuel flammability.

Spatial uncertainty in 21st-century fire regimes

In conjunction with increases in future fire activity, our work also highlights that different areas in Alaska may be more (or less) susceptible to climatically induced changes in fire activity, not only due to varying rates of climate change, but potentially more importantly, due to the proximity of a region (in climate space) to thresholds to burning. Under RCP 6.0, our future projections highlight important changes in the total area and spatial distribution of regions close to the observed temperature threshold to burning (Figure 7), implying spatially varying levels in the uncertainty of our projections. For example, in the early 21st century (i.e., 2010-2039), the average (SD) percentage of Alaskan area projected to lie near the summer-temperature threshold (i.e., $\geq$ 11.4 °C and < 15.4 °C) was 42% (5%), 37% (6%), and 62% (7%) for the GFDL-CM3, IPSL-CM5A, and MRI-CGCM3 GCMs, respectively. Towards the end of the 21st century (2070-2099), more regions are projected to lie well above this threshold, with most areas in Alaska projected to lie 94% (1%), 87% (2%), and 47% (5%) above the temperature threshold for the same three GCMs (i.e., $\geq$ 15.4 °C), respectively.

The uncertainty in future fire activity that is introduced because of threshold-driven fire-climate relationships is strongly dependent on the current climatological location of different regions. Spatial variability in climate implies regionally varying proximity to climate thresholds, and as climate changes throughout the 21st century, these spatial patterns will likewise change. Thus, threshold-related uncertainty in projected fire activity will decrease by the end of the 21st century under RCP 6.0, relative to the early 21st century (Figure 7). This reduced uncertainty by the end of the 21st century is due to most regions of Alaska exceeding climate conditions well above the observed temperature threshold to burning, suggesting fire regimes across Alaska may become most similar to those currently found in the Yukon Flats, the most flammable region of Alaska (Young *et al.* 2017).

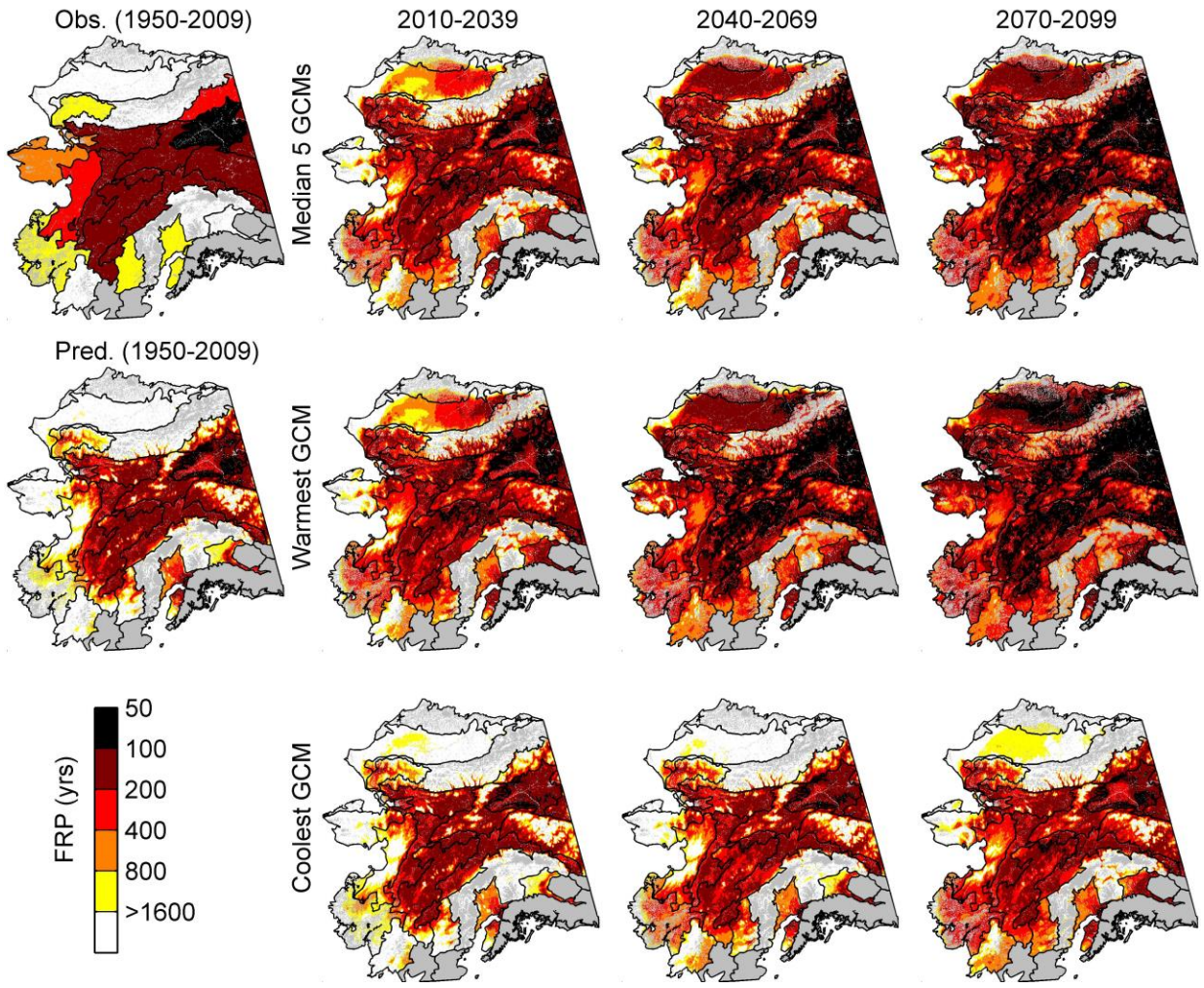

Figure 5. Projected fire rotation periods for three different time periods in the 21st century. The left-most column represents historical observed (first row) and predicted (second row) fire rotation periods in Alaska, as a reference. These projections are for RCP 6.0. This figure was first published in Young *et al.* (2017) as Figure 6.

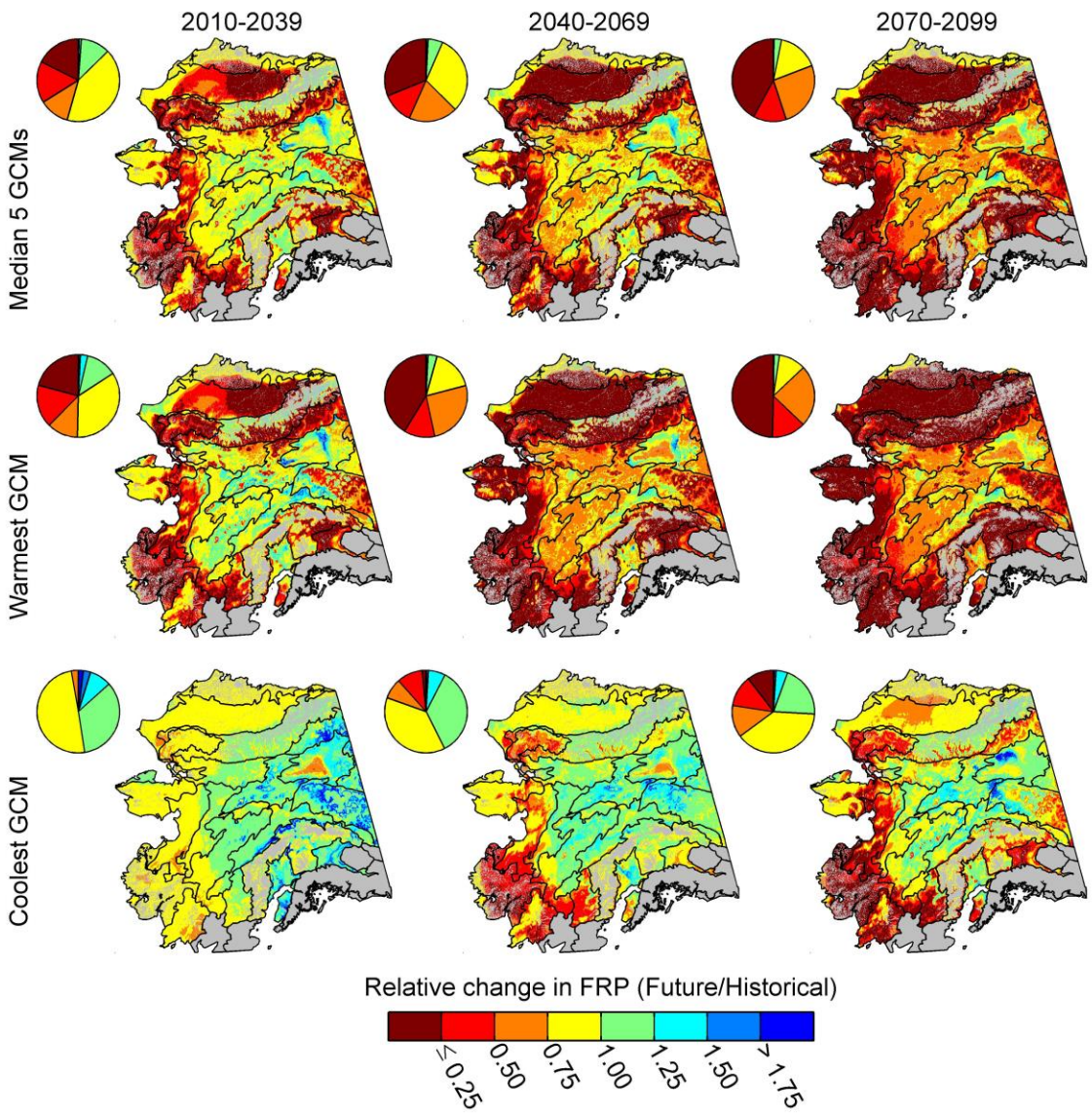

Figure 6. Relative change in the fire rotation period (FRP_{FUTURE} / $FRP_{HISTORICAL}$) per pixel for three different time periods in the 21st century under RCP 6.0. Change is depicted on a nonlinear scale, where a ratio of 0.5 is equal to a 100% increase in area burned, and a ratio 2.0 is equal to a 50% decrease in area burned. Warmer colors indicate an increase in the future probability of fire and thus decreasing fire rotation periods (i.e., relative difference < 1.0); cooler colors indicate a decrease in the future probability of fire and thus increasing fire rotation periods (i.e., relative difference > 1.0). Pie charts depict the proportions of all pixels in the study domain projected to experience a given level of relative change. This figure was first published in Young *et al.* (2017) as Figure 7.

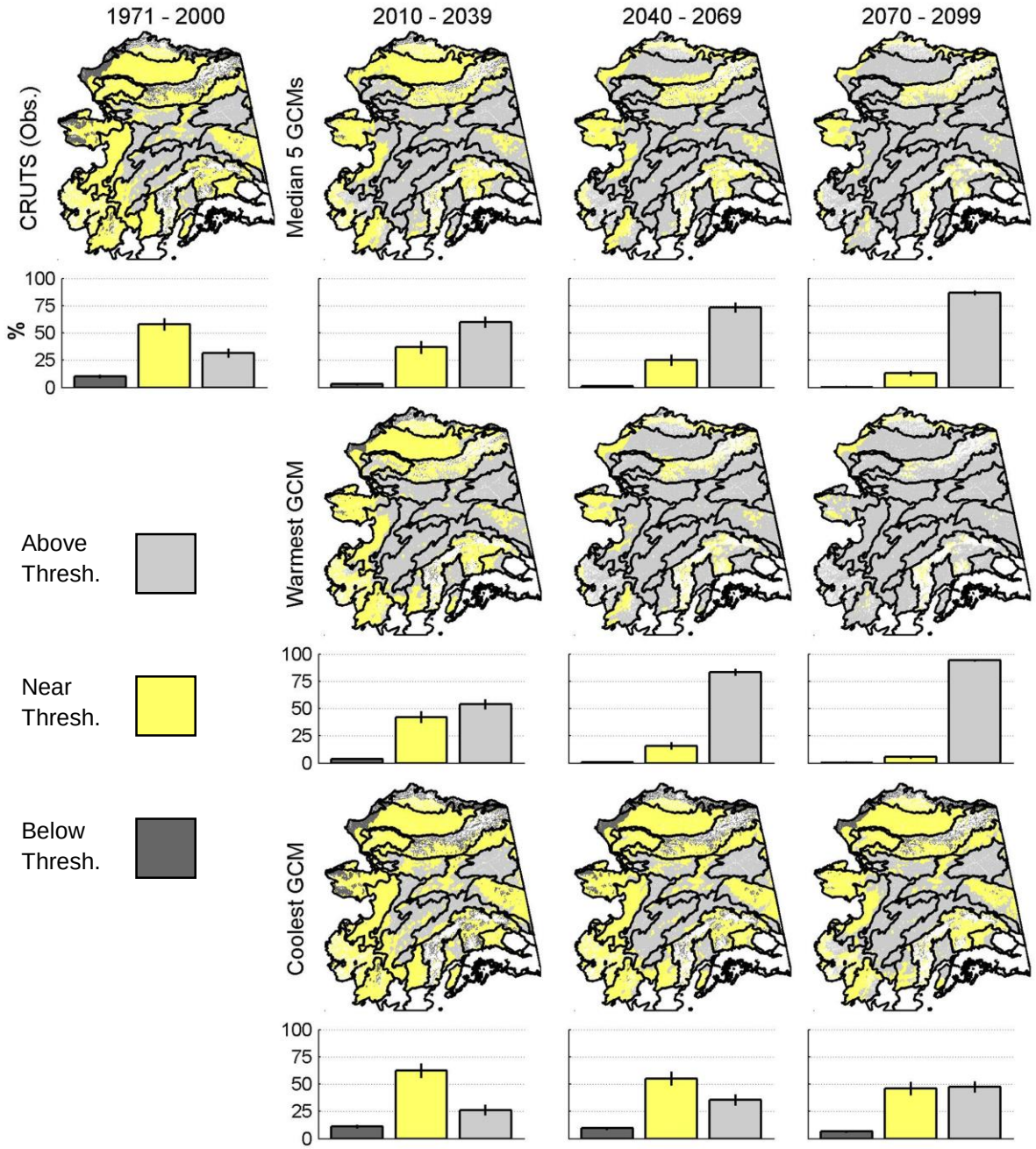

Figure 7. Historical and future distribution of locations in Alaska classified as occurring below, near, or above the 13.4 °C threshold (i.e., within ±2 °C) under the RCP 6.0 scenario. Bar heights indicate the average proportion of each classification (±1 SD), from a random sample of proportions that vary in the classification scheme. Median = IPSL-CM5A-LR, Warmest = GFDL-CM3, Coolest = MRI-CGCM3.

Key findings, implications for management/policy, and future research

A key priority for both scientists and Alaskan land managers is to understand how fire regimes may change in response to 21st-century climate change. Our findings directly address this priority, providing spatially explicit projections of where climate change is expected to make climate conditions more or less conducive to fire activity over the 21st century. We also characterize uncertainty in these future projections, and identify underlying mechanisms driving this prediction uncertainty. Our work highlights how the threshold relationship between climate and fire makes different regions of Alaska more or less vulnerable to climatically induced changes in fire regimes, and it further highlights the uncertainty and challenges associated predicting fire activity beyond the observational record.

Climatic controls of Alaskan fire regimes and vulnerability to 21st-century climate change

Fire activity in Alaskan boreal forest and tundra ecosystems is strongly controlled by climate, with summer temperature emerging as a key determinant of burning, from timescales spanning a single fire season to 30-yr periods defining mean climate conditions (Duffy *et al.* 2005; Balshi *et al.* 2009; Hu *et al.* 2010; Parisien *et al.* 2014; Hu *et al.* 2015; Young *et al.* 2017). This linkage between fire and summer temperatures is due to warmer and drier conditions supporting fire-conducive weather conditions necessary for fuel drying, ignition, and fire spread, and, at longer time scales, warmer summers supporting sufficient biomass to sustain burning. The relationship between temperature and fire is strongly nonlinear, exhibiting a distinct climatic thresholds to burning. This threshold relationship further implies that in some regions of Alaska, relatively small changes in climate could lead to large, sudden shifts fire regimes (Figure 2; Young *et al.* 2017). Together, this tight linkage between fire and climate, as well as the presence of a climatic threshold to burning, implies the potential for significant, climatically induced shifts in fire regimes in Alaska over the course of the 21st-century.

We explored how projected future climate conditions may change fire activity across Alaskan boreal forest and tundra ecosystems by using a set of statistical models and future climate data obtained from GCMs. Under projected warmer temperatures of the 21st century (Appendix H), climate will become increasingly more fire conducive in regions that have burned little in the observational record. In some tundra regions (e.g., Brooks Foothills and Yukon-Kuskokwim Delta ecoregions), our projections suggest shortened fire rotation periods (FRPs) to less than 200 yr, which would be unprecedented in the context of the past 6,000-32,000 yr (Higuera *et al.* 2011b; Chipman *et al.* 2015). For example, compared to mean fire return interval estimates of 4,700 yr for the late Quaternary (Chipman *et al.* 2015), our models suggest an approximately 20-fold decrease in the FRP in the Brooks Foothills. Although our models over predict fire activity in low flammability tundra regions during the historical period (Young *et al.* 2017), even a more conservative 5- to 10-fold decrease in the FRP would represent a substantial increase in fire activity. FRPs are also projected to shorten in most regions of Alaskan boreal forest. Under some projections, future FRPs across most of Alaskan boreal forest may reduce to 50-100 yr, levels similar to the most flammable regions of Alaska over the observational records (i.e., 1950-present; Yukon Flats ecoregion) (Figure 5; Young *et al.* 2017).

While projected increases in fire activity under 21st century warming is consistent with a number of other studies (Balshi *et al.* 2009; Hu *et al.* 2015), the second key finding from this research is elucidating how changes in fire activity may vary across space, revealing regions with more or less vulnerability to climatically induced shifts in fire activity. The likelihood that a given region may experience a dramatic fire-regime shift under future climate change is strongly tied to how close that region lies (in climate space) to a natural threshold to burning. Regions close to the climatic threshold to burning are more vulnerable to climatically induced shifts in fire regimes than those further from this threshold. Specifically, tundra and forest-tundra ecosystems are projected to be the most vulnerable to large fire-regime shifts during the 21st-century, indicated by the largest relative changes when compared to the historical period (Figure 6). Such large changes in fire activity in tundra and forest-tundra ecosystems would likely have significant ecological implications. Alaskan tundra and forest-tundra regions are sensitive to other climatically induced ecological changes, including vegetation shifts (Pearson *et al.* 2013) and permafrost thaw (Romanovsky *et al.* 2010). These ecological changes could interact with wildfire to enhance future landscape flammability in tundra and forest-tundra, forming a positive feedback that would accelerate ecosystem shifts, with important implications for northern high-latitude carbon storage. Temperature-induced shrub expansion (Myers-Smith *et al.* 2011) and drier soils due to permafrost thaw could also serve to increase the probability of fire occurrence (Higuera *et al.* 2008). In turn, more frequent and potentially repeat burning would likely accelerate permafrost thaw (Rocha & Shaver 2011) and alter vegetation successional trajectories (Jones *et al.* 2013), further altering soil hydrology and biogeochemical cycling (Mack *et al.* 2011). The impacts of these potential interactions and feedbacks in tundra and forest-tundra may also be manifested at broader spatial scales, as increased burning (Turetsky *et al.* 2011), productivity (Euskirchen *et al.* 2009), and permafrost thaw (Schuur *et al.* 2015) all alter soil and ecosystem carbon storage, and thus influence atmospheric greenhouse gas concentrations.

Key uncertainties in predicting future fire activity

A major finding of this work is that threshold relationships between fire and climate not only lead to varying levels of vulnerability, but by their very nature they also significantly influence our ability to successfully predict fire activity outside the observational record. We found that when applying statistical models developed with observational data to predict fire activity in a new time period (here 850-1850 CE), accuracy was significantly lower in regions near climatic thresholds to burning relative to regions further away from climatic thresholds (Figure 3). Thus, the same regions that we expect to be most vulnerable to climatically induced shifts in fire activity (i.e., tundra, forest-tundra, and cooler boreal forest regions) are also the regions where we have the most uncertainty, due to sensitivity to any data inaccuracies. In this study, we believe the cause of this underlying uncertainty near climatic threshold is due to biases in the GCM-derived climate data for the past millennium. When compared to paleoclimate data, we found that GCM-based summer temperatures were cooler for 850-1850 CE (Appendix I; Wilson *et al.* 2016). These cooler-than-likely temperatures notably shifted predictions further below the summer temperature threshold, resulting in significant underestimation in fire activity for these regions. For example, in the Kobuk Valley, predictions suggest a difference in mean fire return intervals from approximately 170 yr during the observational record (Kasischke *et al.* 2010) to > 1300 yr during 850-1850 CE under GISS-E2-R projections, our top ranked GCM in Alaska (Appendix D), which is inconsistent with the independent paleo-fire-history records

spanning this period. Thus, we found that relatively minor data inaccuracies, in addition changes to fire-climate relationships, could lead to incorrect inferences regarding fire-regime change (Figure 4).

While we cannot perform a similar evaluation for future projections, because the "results" have yet to happen, we can highlight when and where we would expect future projections to be most sensitive to potential data inaccuracies, ultimately resulting in lower overall confidence for a projection of future fire activity. Using future climate change projections, we found that threshold-related uncertainty will vary across space and time in the 21st century. Under the RCP 6.0 scenario during the early 21st century (i.e., 2010-2039), much of our study area is projected to lie relatively close to a climatic threshold (Figure 7), suggesting high uncertainty around projected fire-regime shifts for most of Alaska. These spatial patterns align well with those regions highlighted as the most vulnerable to experiencing a fire-regime shift in the 21st century (i.e., tundra and forest tundra), which is intuitive given that this measure of vulnerability is directly related to crossing a threshold to burning. By the end of the 21st century (i.e., 2070-2099), however, most areas in Alaska no longer lie near the summer-temperature threshold to burning, including tundra and forest tundra regions; this suggests greater confidence in our projections of fire regime change, specifically in the context of threshold-caused uncertainty. Our results highlight the value of quantifying and visualizing spatial patterns in uncertainty for different GCMs and emissions scenarios, as this information can help identify regions and time periods that are most likely to experience fire-regime shifts. This information should be particularly valuable for aiding land managers and policymakers in anticipating future ecosystem change.

More generally, our future projections of Alaskan fire regime also have two additional important limitations. First, our results highlight significant differences that can arise in future projections among different GCMs. For example, the coolest GCM in our ensemble (MRI-CGCM3) suggests that 48% of our study area in Alaska could experience decreased fire activity during the early 21st century; this contrasts with projections from the warmest GCM (GFDL-CM3), which suggests that only 16% of our study area may experience decreased fire activity during time period. These differences among individual GCMs further support the use of multiple GCMs when evaluating future climate-change impacts on wildfire (Moritz *et al.* 2012). Second, our models do not account for future changes in vegetation, permafrost, or lightning ignitions; rather, they solely represent the suitability of climate for sustaining burning. Thus, the models do not account for potential feedbacks among climate, fire, vegetation, or other ecosystem properties (e.g., permafrost thaw) that could mediate the direct link between climate and fire, which is ultimately what our statistical models reflect. Interactions among climate, vegetation, and fire have been highlighted in the recent and more distant past, in both boreal forest and tundra ecosystems (Higuera *et al.* 2009; Johnstone *et al.* 2010; Kelly *et al.* 2013). For example, in North American boreal forests, burning can reduce subsequent landscape flammability for years to decades, by causing a shift from more flammable coniferous forests to less flammable deciduous forests (Kelly *et al.* 2013), or due a reduction in burnable biomass through a shift from landscapes dominated by older to younger forest stands (Héon *et al.* 2014). Thus, the initial climate-induced increases in fire activity during the early 21st century suggested by our projections (e.g., Figure 5) may result in decreased fire activity by mid-century, even if climate becomes more conducive for burning.

Future research needs

This work helps identify several research needs that would continue to advance our ability to anticipate and predict how fire regimes may shift during the course of the 21st century. First, more research is needed to understand what factors can mediate the strong linkages between climate and fire highlighted in this and previous work. The potential for changing fire-climate relationships under future climatic and environmental conditions would have important implications for anticipating future fire-regime shifts. As vegetation changes, either in response to climate and/or disturbance, fire-climate relationships observed during the past half century may or may not change (e.g., Duffy *et al.* 2014). Understanding this potential for altered fire-climate relationships in the future, and how these changes may impact future patterns in fire activity, will require exploring how fire-climate relationships vary among different vegetation communities, and across different spatial and temporal scales Additionally, predicting the direct impacts of climate change on vegetation communities (e.g., Pearson *et al.* 2013) will also be key for understanding the consequences of future climate change for fire regimes in Alaska. Therefore, future research should focus on integrating the coupled relationships among climate, fire, and vegetation to develop more robust future projections of fire activity. Ultimately, this is what is needed to provide more precise understanding of the timing, location, and magnitude of potential fire-regime shifts in boreal forest and tundra ecosystems.

Literature Cited

Aertsen, W., Kint, V., van Orshoven, J., Ozkan, K. & Muys, B. (2010). Comparison and ranking of different modelling techniques for prediction of site index in Mediterranean mountain forests. *Ecol. Model.*, 221, 1119-1130.

Austin, M.P., Nicholls, A.O. & Margules, C.R. (1990). Measurement of the Realized Qualitative Niche - Environmental Niches of 5 Eucalyptus Species. *Ecol. Monogr.*, 60, 161-177.

Balshi, M.S., McGuire, A.D., Duffy, P., Flannigan, M., Walsh, J. & Melillo, J. (2009). Assessing the response of area burned to changing climate in western boreal North America using a Multivariate Adaptive Regression Splines (MARS) approach. *Global Change Biol.*, 15, 578-600.

Barrett, C.M., Kelly, R., Higuera, P.E. & Hu, F.S. (2013). Climatic and land cover influences on the spatiotemporal dynamics of Holocene boreal fire regimes. *Ecology*, 94, 389-402.

Barry, S. & Elith, J. (2006). Error and uncertainty in habitat models. *J. Appl. Ecol.*, 43, 413-423.

Biggs, R., Carpenter, S.R. & Brock, W.A. (2009). Turning back from the brink: Detecting an impending regime shift in time to avert it. *Proc. Natl. Acad. Sci. USA*, 106, 826-831.

Braconnot, P., Harrison, S.P., Kageyama, M., Bartlein, P.J., Masson-Delmotte, V., Abe-Ouchi, A. *et al.* (2012). Evaluation of climate models using palaeoclimatic data. *Nat. Clim. Change*, 2, 417-424.

Chipman, M.L., Hudspith, V., Higuera, P.E., Duffy, P.A., Kelly, R., Oswald, W.W. *et al.* (2015). Spatiotemporal patterns of tundra fires: Late-Quaternary charcoal records from Alaska. *Biogeosciences*, 12, 4017-4027.

Diniz-Filho, J.A., Bini, L.M., Rangel, T.F., Loyola, R.D., Hof, C., Nogues-Bravo, D. *et al.* (2009). Partitioning and mapping uncertainties in ensembles of forecasts of species turnover under climate change. *Ecography*, 32, 897-906.

Duffy, P.A., Walsh, J.E., Graham, J.M., Mann, D.H. & Rupp, T.S. (2005). Impacts of large-scale atmospheric-ocean variability on Alaskan fire season severity. *Ecol. Appl.*, 15, 1317-1330.

Duffy, P., Higuera, P.E., Young, A.M., Dietze, M.C. & Hu, F.S. (2014). Mediation of fire-climate linkages by vegetation types in Alaskan arctic tundra ecosystems: impacts of model uncertainty on GCM-based forecasts of future fire activity. In: *American Geophysical Union Fall Meeting* San Francisco, CA, 15-19 December, B51H-0118.

Elith, J., Burgman, M.A. & Regan, H.M. (2002). Mapping epistemic uncertainties and vague concepts in predictions of species distribution. *Ecol. Model.*, 157, 313-329.

Elith, J. & Leathwick, J.R. (2009). Species distribution models: Ecological explanation and prediction across space and time. *Annu. Rev. Ecol. Evol. S.*, 40, 677-697.

Euskirchen, E.S., McGuire, A.D., Chapin, F.S., Yi, S. & Thompson, C.C. (2009). Changes in vegetation in northern Alaska under scenarios of climate change, 2003-2100: implications for climate feedbacks. *Ecol. Appl.*, 19, 1022-1043.

Flannigan, M.D. & Harrington, J.B. (1988). A Study of the Relation of Meteorological Variables to Monthly Provincial Area Burned by Wildfire in Canada (1953-80). *Journal of Applied Meteorology*, 27, 441-452.

Friedman, J.H. (2001). Greedy function approximation: A gradient boosting machine. *Ann. Stat.*, 29, 1189-1232.

Friedman, J.H. (2002). Stochastic gradient boosting. *Comput. Stat. Data. An.*, 38, 367-378.

Giorgi, F. & Mearns, L.O. (1991). Approaches to the simulation of regional climate change - a review. *Rev. Geophys.*, 29, 191-216.

Graham, C.H., Ron, S.R., Santos, J.C., Schneider, C.J. & Moritz, C. (2004). Integrating phylogenetics and environmental niche models to explore speciation mechanisms in dendrobatid frogs. *Evolution*, 58, 1781-1793.

Grimm, N.B., Chapin, F.S., Bierwagen, B., Gonzalez, P., Groffman, P.M., Luo, Y.Q. *et al.* (2013). The impacts of climate change on ecosystem structure and function. *Front. Ecol. Environ.*, 11, 474-482.

Guisan, A. & Zimmermann, N.E. (2000). Predictive habitat distribution models in ecology. *Ecol. Model.*, 135, 147-186.

Gunderson, L.H. (2000). Ecological resilience - in theory and application. *Annu Rev Ecol Syst*, 31, 425-439.

Heikkinen, R.K., Luoto, M., Araujo, M.B., Virkkala, R., Thuiller, W. & Sykes, M.T. (2006). Methods and uncertainties in bioclimatic envelope modelling under climate change. *Prog. Phys. Geog.*, 30, 751-777.

Héon, J., Arseneault, D. & Parisien, M.A. (2014). Resistance of the boreal forest to high burn rates. *Proc. Natl. Acad. Sci. USA*, 111, 13888-13893.

Higuera, P.E., Abatzoglou, J.T., Littell, J.S. & Morgan, P. (2015). The Changing Strength and Nature of Fire-Climate Relationships in the Northern Rocky Mountains, USA, 1902-2008. *Plos One*, 10.

Higuera, P.E., Brubaker, L.B., Anderson, P.M., Brown, T.A., Kennedy, A.T. & Hu, F.S. (2008). Frequent Fires in Ancient Shrub Tundra: Implications of Paleorecords for Arctic Environmental Change. *Plos One*, 3, e0001744.

Higuera, P.E., Brubaker, L.B., Anderson, P.M., Hu, F.S. & Brown, T.A. (2009). Vegetation mediated the impacts of postglacial climate change on fire regimes in the south-central Brooks Range, Alaska. *Ecol. Monogr.*, 79, 201-219.

Higuera, P.E., Chipman, M.L., Barnes, J.L., Urban, M.A. & Hu, F.S. (2011a). Variability of tundra fire regimes in Arctic Alaska: millennial scale patterns and ecological implications. *Ecol. Appl.*, 21, 3211-3226.

Higuera, P.E., Barnes, J.L., Chipman, M.L., Urban, M. & Hu, F.S. (2011b). Tundra fire history over the past 6000 years in the Noatak National Preserve, northwestern Alaska. *Alaska Park Science*, 10, 37-41.

Hu, F.S., Higuera, P.E., Duffy, P., Chipman, M.L., Rocha, A.V., Young, A.M. *et al.* (2015). Arctic tundra fires: natural variability and responses to climate change. *Front. Ecol. Environ.*, 13, 369-377.

Hu, F.S., Higuera, P.E., Walsh, J.E., Chapman, W.L., Duffy, P.A., Brubaker, L.B. *et al.* (2010). Tundra burning in Alaska: Linkages to climatic change and sea ice retreat. *J. Geophys. Res.-Biogeo.*, 115, G04002.

Jacobson, G.L. (1988). Ancient permanent plots: Sampling in paleovegetational studies. In: *Vegetation history* (eds. Huntley, B & Webb, T). Kluwer Academic Publishers, pp. 1-16.

Johnson, E.A. & Gutsell, S.L. (1994). Fire frequency models, methods and interpretations. *Adv. Ecol. Res.*, 25, 239-287.

Johnstone, J.F., Chapin, F.S., Hollingsworth, T.N., Mack, M.C., Romanovsky, V. & Turetsky, M. (2010). Fire, climate change, and forest resilience in interior Alaska. *Can. J. Forest Res.*, 40, 1302-1312.

Jones, B.M., Breen, A.L., Gaglioti, B.V., Mann, D.H., Rocha, A.V., Grosse, G. *et al.* (2013). Identification of unrecognized tundra fire events on the north slope of Alaska. *J. Geophys. Res.-Biogeo.*, 118, 1334-1344.

Kasischke, E.S., Verbyla, D.L., Rupp, T.S., McGuire, A.D., Murphy, K.A., Jandt, R. *et al.* (2010). Alaska's changing fire regime - implications for the vulnerability of its boreal forests. *Can. J. Forest Res.*, 40, 1313-1324.

Kasischke, E.S., Williams, D. & Barry, D. (2002). Analysis of the patterns of large fires in the boreal forest region of Alaska. *Int. J. Wildland Fire*, 11, 131-144.

Kefi, S., Dakos, V., Scheffer, M., Van Nes, E.H. & Rietkerk, M. (2013). Early warning signals also precede non-catastrophic transitions. *Oikos*, 122, 641-648.

Kelly, R., Chipman, M.L., Higuera, P.E., Stefanova, I., Brubaker, L.B. & Hu, F.S. (2013). Recent burning of boreal forests exceeds fire regime limits of the past 10,000 years. *Proc. Natl. Acad. Sci. USA*, 110, 13055-13060.

Krawchuk, M.A. & Moritz, M.A. (2014). Burning issues: statistical analyses of global fire data to inform assessments of environmental change. *Environmetrics*, 25, 472-481.

Krawchuk, M.A., Moritz, M.A., Parisien, M.A., Van Dorn, J. & Hayhoe, K. (2009). Global Pyrogeography: the Current and Future Distribution of Wildfire. *Plos One*, 4.

Mack, M.C., Bret-Harte, M.S., Hollingsworth, T.N., Jandt, R.R., Schuur, E.A.G., Shaver, G.R. *et al.* (2011). Carbon loss from an unprecedented Arctic tundra wildfire. *Nature*, 475, 489-492.

Martínez-Meyer, E., Townsend Peterson, A. & Hargrove, W.W. (2004). Ecological niches as stable distributional constraints on mammal species, with implications for Pleistocene extinctions and climate change projections for biodiversity. *Global Ecol. Biogeogr.*, 13, 305-314.

McAfee, S.A. (2013). Methodological differences in projected potential evapotranspiration. *Climatic Change*, 120, 915-930.

Moreno-Amat, E., Mateo, R.G., Nieto-Lugilde, D., Morueta-Holme, N., Svenning, J.C. & Garcia-Amorena, I. (2015). Impact of model complexity on cross-temporal transferability in Maxent species distribution models: An assessment using paleobotanical data. *Ecol. Model.*, 312, 308-317.

Moritz, M.A., Parisien, M.A., Batllori, E., Krawchuk, M.A., Van Dorn, J., Ganz, D.J. *et al.* (2012). Climate change and disruptions to global fire activity. *Ecosphere*, 3: art49.

Muggeo, V.M.R. (2003). Estimating regression models with unknown break-points. *Stat. Med.*, 22, 3055-3071.

Myers-Smith, I.H., Forbes, B.C., Wilmking, M., Hallinger, M., Lantz, T., Blok, D. *et al.* (2011). Shrub expansion in tundra ecosystems: dynamics, impacts and research priorities. *Environ Res Lett*, 6.

Nowacki, G., Spencer, P., Brock, T., Fleming, M. & Jorgenson, T. (2001). Ecoregions of Alaska and neighboring territories - US Geological Survey Open-File Report 02-297 (map). Online at http://agdc.usgs.gov/data/projects/fhm/#H, USGS Reston, VA.

Parisien, M.A., Parks, S.A., Krawchuk, M.A., Little, J.M., Flannigan, M.D., Gowman, L.M. *et al.* (2014). An analysis of controls on fire activity in boreal Canada: Comparing models built with different temporal resolutions. *Ecol. Appl.*, 24, 1341-1356.

Pausas, J.G. & Paula, S. (2012). Fuel shapes the fire-climate relationship: evidence from Mediterranean ecosystems. *Global Ecol. Biogeogr.*, 21, 1074-1082.

Pearson, R.G., Phillips, S.J., Loranty, M.M., Beck, P.S.A., Damoulas, T., Knight, S.J. *et al.* (2013). Shifts in Arctic vegetation and associated feedbacks under climate change. *Nat. Clim. Change*, 3, 673-677.

Peters, D.P.C., Herrick, J.E., Urban, D.L., Gardner, R.H. & Breshears, D.D. (2004a). Strategies for ecological extrapolation. *Oikos*, 106, 627-636.

Peters, D.P.C., Pielke, R.A., Bestelmeyer, B.T., Allen, C.D., Munson-McGee, S. & Havstad, K.M. (2004b). Cross-scale interactions, nonlinearities, and forecasting catastrophic events. *Proc. Natl. Acad. Sci. USA*, 101, 15130-15135.

Randin, C.F., Dirnbock, T., Dullinger, S., Zimmermann, N.E., Zappa, M. & Guisan, A. (2006). Are niche-based species distribution models transferable in space? *Journal of Biogeography*, 33, 1689-1703.

Regan, H.M., Colyvan, M. & Burgman, M.A. (2002). A taxonomy and treatment of uncertainty for ecology and conservation biology. *Ecol. Appl.*, 12, 618-628.

Rocha, A.V. & Shaver, G.R. (2011). Postfire energy exchange in arctic tundra: the importance and climatic implications of burn severity. *Global Change Biol.*, 17, 2831-2841.

Romanovsky, V.E., Smith, S.L. & Christiansen, H.H. (2010). Permafrost Thermal State in the Polar Northern Hemisphere during the International Polar Year 2007-2009: a Synthesis. *Permafrost Periglac*, 21, 106-116.

Rupp, D.E., Abatzoglou, J.T., Hegewisch, K.C. & Mote, P.W. (2013). Evaluation of CMIP5 20th century climate simulations for the Pacific Northwest USA. *J. Geophys. Res.-Atmos.*, 118, 10884-10906.

Scenarios Network for Alaska and Arctic Planning, University of Alaska. 2015. Projected Monthly Temperature and Precipitation - 2 km CMIP5/AR5. Retrieved January 2015 from https://www.snap.uaf.edu/tools/data-downloads.

Scheffer, M., Bascompte, J., Brock, W.A., Brovkin, V., Carpenter, S.R., Dakos, V. *et al.* (2009). Early-warning signals for critical transitions. *Nature*, 461, 53-59.

Schuur, E.A.G., McGuire, A.D., Schadel, C., Grosse, G., Harden, J.W., Hayes, D.J. *et al.* (2015). Climate change and the permafrost carbon feedback. *Nature*, 520, 171-179.

Taylor, K.E., Stouffer, R.J. & Meehl, G.A. (2012). An overview of CMIP5 and the experiment design. *B. Am. Meteorol. Soc.*, 93, 485-498.

Thomas, J.A. & Bovee, K.D. (1993). Application and Testing of a Procedure to Evaluate Transferability of Habitat Suitability Criteria. *Regul River*, 8, 285-294.

Turetsky, M.R., Kane, E.S., Harden, J.W., Ottmar, R.D., Manies, K.L., Hoy, E. *et al.* (2011). Recent acceleration of biomass burning and carbon losses in Alaskan forests and peatlands. *Nat. Geosci.*, 4, 27-31.

Turner, M.G. & Romme, W.H. (1994). Landscape dynamics in crown fire ecosystems. *Landscape Ecol.*, 9, 59-77.

Walther, G.R., Post, E., Convey, P., Menzel, A., Parmesan, C., Beebee, T.J.C. *et al.* (2002). Ecological responses to recent climate change. *Nature*, 416, 389-395.

Watling, J.I., Brandt, L.A., Bucklin, D.N., Fujisaki, I., Mazzotti, F.J., Romanach, S.S. *et al.* (2015). Performance metrics and variance partitioning reveal sources of uncertainty in species distribution models. *Ecol. Model.*, 309, 48-59.

Wenger, S.J. & Olden, J.D. (2012). Assessing transferability of ecological models: an underappreciated aspect of statistical validation. *Methods Ecol. Evol.*, 3, 260-267.

Wenger, S.J., Som, N.A., Dauwalter, D.C., Isaak, D.J., Neville, H.M., Luce, C.H. *et al.* (2013). Probabilistic accounting of uncertainty in forecasts of species distributions under climate change. *Global Change Biol.*, 19, 3343-3354.

Williams, A.P. & Abatzoglou, J. (2016). Recent advances and remaining uncertainties in resolving past and future climate effects on global fire activity. *Current Climate Change Reports*, 2, 1-14.

Wilson, R., Anchukaitis, K., Briffa, K.R., Buntgen, U., Cook, E., D'Arrigo, R. *et al.* (2016). Last millennium northern hemisphere summer temperatures from tree rings: Part I: The long term context. *Quat. Sci. Rev.*, 134, 1-18.

Young, A.M., Higuera, P.E., Duffy, P.A. & Hu, F.S. (2017). Climatic thresholds shape northern high-latitude fire regimes and imply vulnerability to future change. *Ecography*, 40, 606-617.

Appendix A: Contact Information for Key Project Personnel

Investigators

Dr. Luigi Boschetti (PI)
Associate Professor
College of Natural Resources
University of Idaho
Moscow, ID 83844
email: luigi [at] uidaho.edu
phone: 208.885.6508

Dr. Philip E. Higuera (Co-PI)*
Associate Professor
Dept. of Ecosystem and Conservation Sciences
University of Montana
Missoula, MT 59812
email: philip.higuera [at] umontana.edu
phone: 406.243.6337
**Original PI prior to moving institutions; point of contact for project inquiries.*

Adam M. Young, M.S. (Student Investigator)
Ph.D. Candidate
Dept. Forest, Rangeland, and Fire Sciences
University of Idaho
Moscow, ID 83844
email: amyoung [at] uidaho.edu
phone: N/A

Collaborators

Dr. John Abatzoglou
Associate Professor
Dept. of Geography
University of Idaho
Moscow, ID 83844
email: jabatzoglou [at] uidaho.edu
phone: 208.885.6239

Dr. Paul Duffy
Neptune and Company, Inc.
Lakewood, CO 80215
email: paul.duffy [at] neptune.org
phone: 970.416.6488

Dr. Feng Sheng Hu
Associate Dean, College of Liberal Arts and Sciences
Professor, Department of Plant Biology
Ralph E. Grim Professor, Department of Geology
Professor, Program in Ecology, Evolution, and Conservation Biology
University of Illinois
Urbana, IL 61801
email: fshu [at] life.illinois.edu
phone: 217.300.9440

Appendix B: List of Completed/Planned Publications/Science Delivery Products

Deliverable type	Product
Datasets	Young, A. M., P. E. Higuera, P. A. Duffy, and F. S. Hu. 2016. Data from: Climatic thresholds shape northern high-latitude fire regimes and imply vulnerability to future climate change. Dryad Digital Repository. doi: 10.5061/dryad.r217r
Dissertation	Young, A. M. *In Prep.* Sensitivity of past, present, and future fire regimes to climate and vegetation variability in boreal forest and tundra ecosystems. University of Idaho, Moscow, ID.
Guest lectures	Young, A. M. 2016. Introduction to fire-climate relationships: concepts and applications. Basic and Applied Fire Ecology (Course: FORS 333). University of Montana, Missoula, MT. Young, A. M. 2016. Fire in the Far North: tundra and boreal forests. Basic and Applied Fire Ecology (Course: FORS 333). University of Montana, Missoula, MT.
Refereed publications	In preparation: Young, A. M., P. E. Higuera, J. Abatzoglou, P. A. Duffy, and F. S. Hu. *In Prep*. Consequences of threshold relationships for predicting ecological change. Published: Young, A. M., P. E. Higuera, P. A. Duffy, and F.S. Hu. 2017. Climatic thresholds shape northern high-latitude fire regimes and imply vulnerability to future climate change. *Ecography*, 40: 606-627. doi: 10.1111/ecog.02205
Professional presentations	Young, A. M., P. E. Higuera, J. Abatzoglou, P. A. Duffy, and F. S. Hu. 2016. Predicting fire-regime responses to climate change over the past millennium: Implications of paleodata-model comparisons for future projections of fire activity. American Geophysical Union Fall Meeting, San Francisco, USA. (Poster) Young, A. M., P. E. Higuera, P. A. Duffy, L. Boschetti, and F. S. Hu. 2014. Climatic controls of wildfire in the boreal forest and arctic tundra biomes across multiple spatial and temporal Scales. American Geophysical Union Fall Meeting, San Francisco, USA. (Oral)
Public presentations	Young, A. M., P. E. Higuera, J. Abatzoglou, P. A. Duffy, and F. S. Hu. 2017. Implications of threshold relationships for projecting fire-regime responses to climate change. Alaska Fire Science Consortium Webinar. April 25, 2017.

Appendix C: *Metadata*

With the submission of this final report, we also provide metadata for the downscaled-GCM data used to conduct this research. Given the synthesis nature of this research, most of the data we use are already published and publicly available, with the exception of the downscaled climate data. Thus, as described in our Data Management Plan, we will provide methods and examples for the downscaling GCM data. The downscaled-GCM data generated in this project provide projections of monthly mean temperature and total precipitation at a 2-km spatial resolution for mainland Alaska from 850-2100 CE. The intended purpose of these downscaled data is to inform and drive a set of existing statistical models to predict the spatially explicit probability of fire occurrence at 30-yr timescales. Details regarding the downscaling of this data are described in the "Materials and Methods" section and Appendix E in this report. These data will be made publicly available either once the research has been published, or within two years of project completion (i.e., 06/30/2017), whichever comes first. When ready, the data will be archived in USFS Research Data Archive (https://www.fs.usda.gov/rds/archive/).

Appendix D: *Ranking Global Climate Model (GCM) performance in Alaska*

GCM and observational data

The goal of this ranking analysis was to select global climate models (GCMs) that were most skillful at predicting July temperature and total annual precipitation in mainland Alaska, thus allowing us to inform our statistical models with the best available GCM estimates outside of the observational record, in the past or future. Here, GCM skill was assessed through comparisons with observed climate from 1951-2000 CE. We chose 1951-2000 as the time period for these comparisons, as observed datasets were unnaturally homogenous across space prior to 1950, due to a lack of climate station information. For each GCM and observed dataset combination, performance was measured by comparing observed and GCM-derived July monthly surface air temperature and total annual precipitation. Our focus is on these two climate variables because they are also those used that inform our statistical models. The GCMs considered in this ranking analysis were chosen from the Earth System Grid Federation (https://www.earthsystemcog.org/projects/cog/) under the following criteria, they: (1) provided estimates for surface air temperature (tas) and precipitation (pr), (2) were at a monthly time frequency, and (3) were available for the past millennium (850 – 1850 CE), the historical period (1851 – 2005 CE), and in 21st-century projections under the RCP 4.5 and RCP 8.5 scenarios (2006 – 2100 CE).

Observed climate data, used for comparison with GCMs, were obtained from three sources: (1) climate research unit time series data version 3.23 (CRUTS323, Harris *et al.* 2014), (2) time series data from the University of Delaware (UDelaware; Willmott & Matsuura 2012, temperature: http://climate.geog.udel.edu/~climate/html_pages/Global2011/README.GlobalTsT2011.html, precipitation: http://climate.geog.udel.edu/~climate/html_pages/Global2011/Precip_revised_3.02/README.GlobalTsP2011.html), and (3) monthly mean forecast data from the ECMWF 20th-Century Reanalysis (ERA20C; Poli *et al.* [2016]; https://www.ecmwf.int/en/research/climate-reanalysis/era-20c). Additional details for these observed data are listed in Table D1.

Quantifying GCM performance

To understand GCM performance in Alaska, we chose a set of performance metrics (Table D2; based off of those presented in Rupp *et al.* [2013]), designed to evaluate how well GCMs simulated: (1) spatial patterns, (2) seasonal climate, (3) climatic trends, and (4) temporal variability. Prior to evaluating these metrics, we first resampled each GCM and observed dataset using bilinear interpolation to a common spatial resolution of 2°×2°. To evaluate spatial patterns, we took 50-yr climatological normals (i.e., (1951-2000) for each individual grid cell and calculated the linear correlations between each GCM and observed dataset, treating each pixel as an observation. To evaluate seasonal climate, we calculated the root mean square error (*RMSE*, Eqn. D1) between observed and predicted monthly climatological normals. Here, we averaged across all pixels in mainland Alaska and all 50 yr, thus providing a single value for each month and variable in Alaska. Specifically, for the j^{th} GCM, the *RMSE* was defined as

$$RMSE_j = \sqrt{n^{-1}\sum_{i=1}^{n}\left(x_{i,j} - x_{i,obs}\right)^2} \quad \text{(D1)}$$

Here, n is equal to the number of months, $x_{i,j}$ is the GCM-derived estimate for the i^{th} month, and $x_{i,obs}$ is the observed. Prior to calculating *RMSE*, monthly climatic averages were standardized by subtracting (dividing) the 1951-2000 12-month average for temperature (total precipitation). Trends in climate change for 1951-2000 were calculated by averaging across all months and grid points for each individual year from 1950-1999, and then estimating the slope parameter from a simple linear regression between year and climate. Finally, to measure temporal variability, we calculated two different metrics: standard deviation (*SD*) for temperature and the coefficient of variation (i.e., $CV = SD/\bar{x}$) for precipitation, at two different timescales: annual and decadal.

To quantify GCM performance, we used a relative error metric (Eqn. D2; defined in Rupp *et al.* [2013]). This metric normalizes a measure of absolute error between GCM and observed estimates. To calculate relative error for a given metric, first, absolute error is calculated

$$e_{i,j} = \left|x_{i,j} - x_{i,obs}\right|$$

Here, $x_{i,j}$ is the j^{th} GCM-estimate for the i^{th} of ten metrics (Table D2), and $x_{i,obs}$ is the estimate for a given observed dataset. This absolute error is normalized

$$e^*_{i,j} = \frac{e_{i,j} - \min(E)}{\max(E) - \min(E)} \quad \text{(D2)}$$

Here, E is a set of the n absolute error values from all performance metrics (i.e., $E = \{e_{1,j}, e_{2,j}, ..., e_{n,j}\}$). For each observed dataset, each GCM was given a total relative error score, equal to the total summation across of ten performance metrics

$$E_{tot,j} = \sum_{i=1}^{10} e^*_{i,j}$$

Finally, the average relative error was calculated summed across all observed datasets (i.e., n = 3), proving a single metric of relative performance for each GCM (Table D3).

Summary of ranking results

From our ranking analysis, the GISS-E2-R had the best overall performance, with an average (SD) total relative error score of 3.24 (0.71) (Table D3). Comparatively, the GCMs with the next-best performances were the MPI-ESM-P and MRI-CGCM3, with average (SD) total relative error scores of 3.79 (1.34) and 4.38 (0.63), respectively (Table D3). The MIROC-ESM appeared to have the lowest overall performance among all five GCMs, with an average (SD) total relative error score of 6.85 (0.65) (Table D3). To aid in evaluation of the relative performance of each GCM, we proved visualizations depicting GCM- and observationally derived estimates for climatic spatial patterns (Figures D1 & D2), seasonal climate (Figure D3), annual trends (Figure D4), temporal variability (Figure D5), as well as the relative error score for each of these metrics (Figure D6).

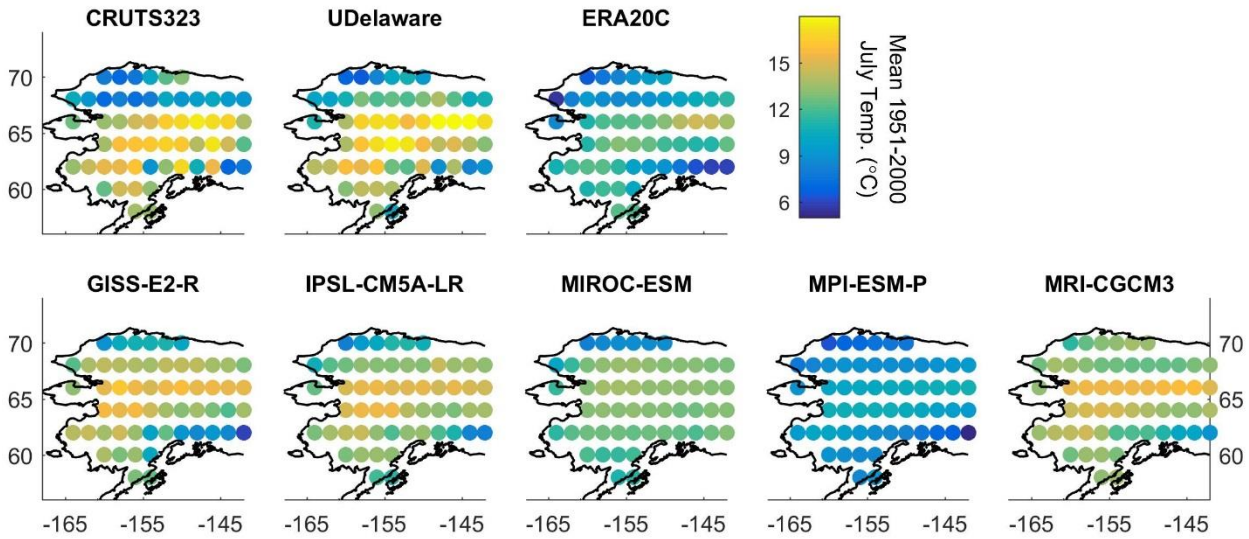

Figure D1. Spatial patterns in mean July temperature (1951-2000) obtained from observed (first row) and GCM (second row) estimates.

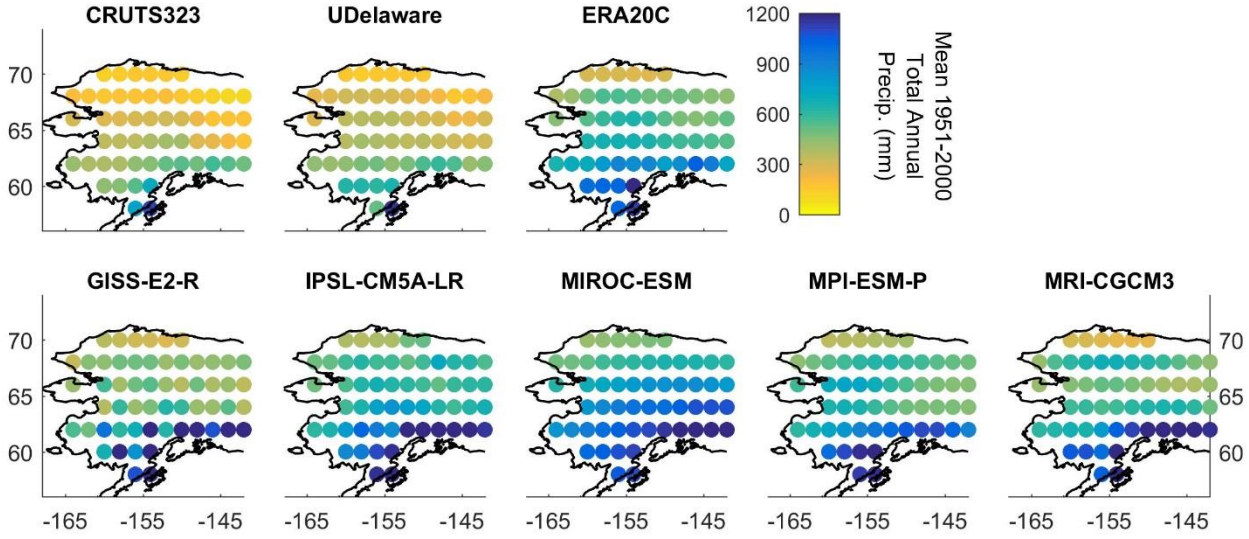

Figure D2. Spatial patterns in mean total annual precipitation (1951-2000) obtained from observed (first row) and GCM (second row) estimates.

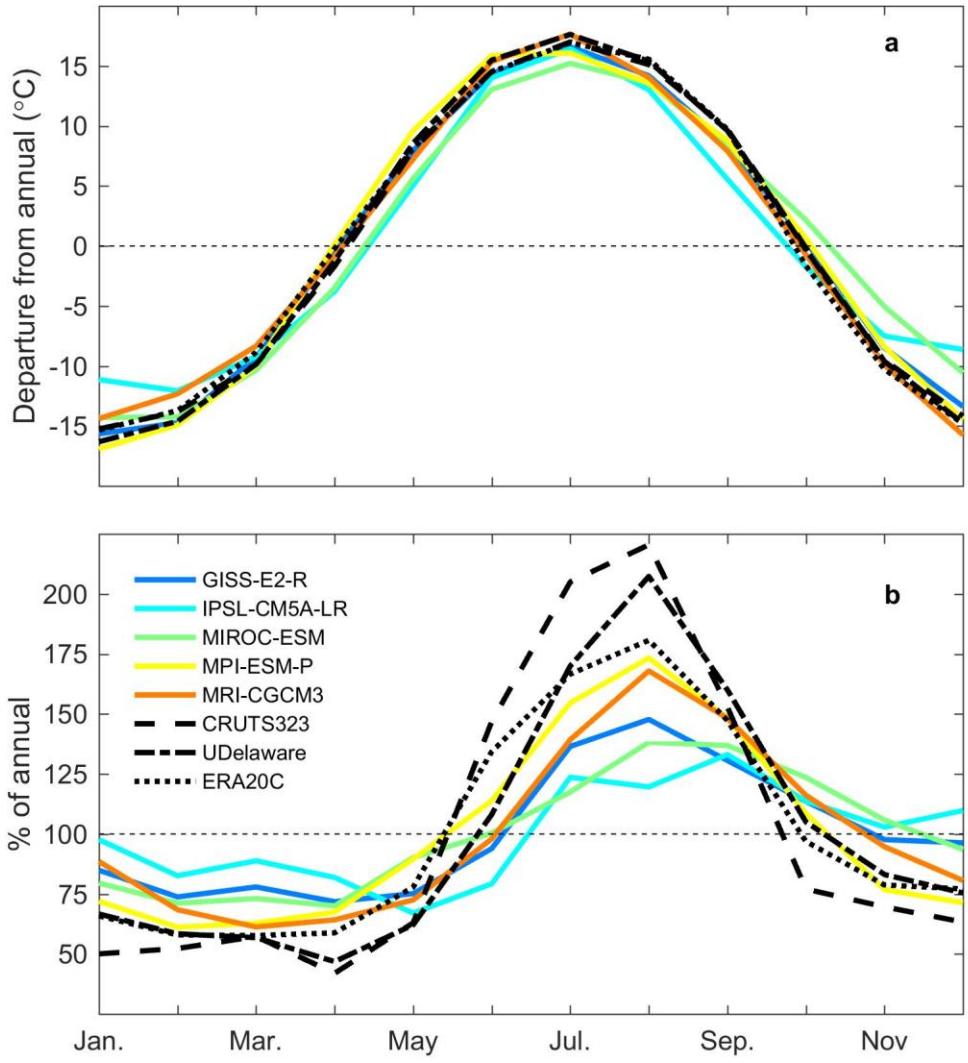

Figure D3. Average seasonal climatological patterns of (a) monthly mean temperature and (b) total precipitation (1951-2000).

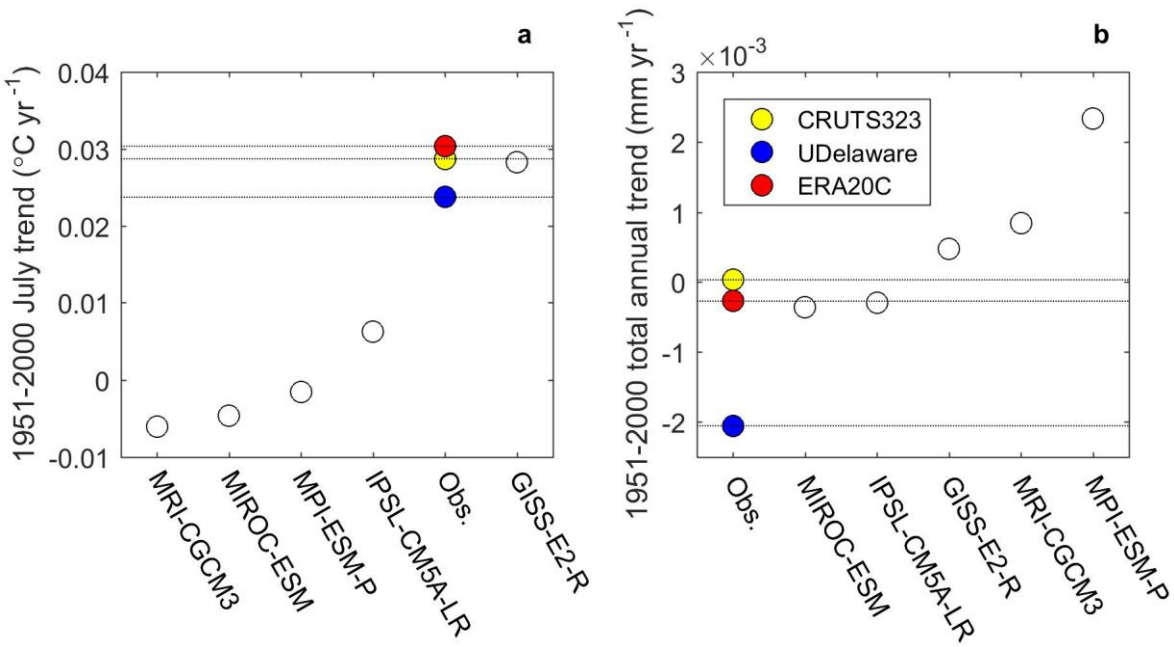

Figure D4. Fifty-year linear trends for (a) July temperature and (b) total annual precipitation.

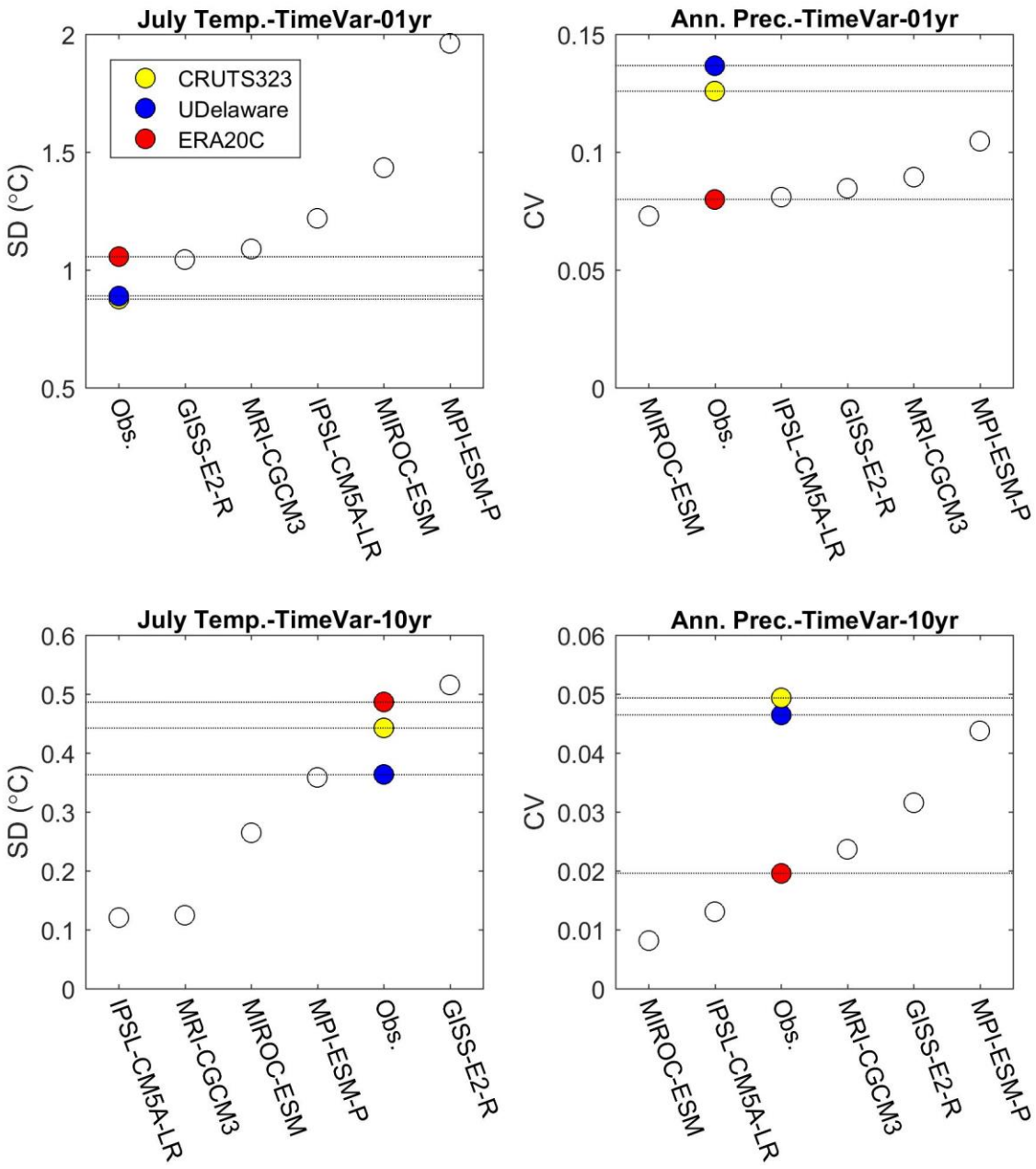

Figure D5. Annual (top row) and decadal (bottom row) variability for July temperature (left column) and total annual precipitation (right column), 1951-2000.

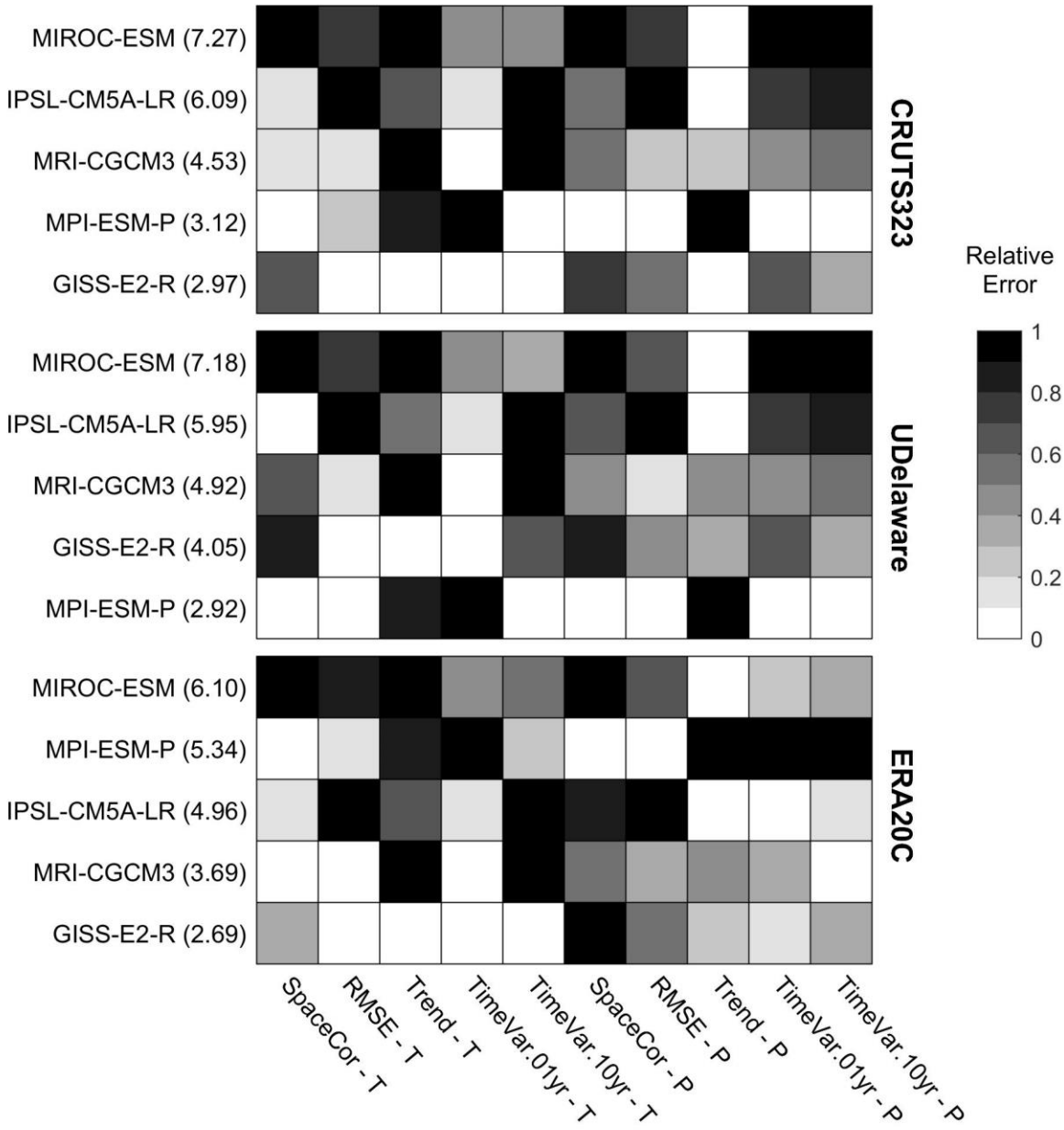

Figure D6. Relative error for each metric and GCM among all three observational datasets. The relative error for each metric is unitless and on a scale from 0-1. For each observational dataset, GCMs are listed in the rows in descending order from least-to-most skillful, according to the total relative error (highlighted in parentheses).

Table D1. Details for the five GCMs used in our ranking analysis and the 3 observed datasets. All GCMs are under the first ensemble member (i.e., r1i1p1), expect GISS-E2-R (r1i1p124).

	Dataset name	Source	Spatial resolution (Lon. × Lat.)	Temporal coverage past1000/historical (yyyymm)
Observed	CRUTS323	Climate Research Unit Time Series version 3.23, University of East Anglia	0.5 × 0.5	NA/ 190101-201412
	UDelaware	Gridded Monthly Time Series Data version 3.01 (temp) and 3.02 (precip), University of Delaware	0.5 × 0.5	NA/ 190001-201412
	ERA20C	European Centre for Medium-Range Weather Forecasts	1.0 × 1.0	NA/ 190001-201012
GCM	GISS-E2-R	NASA Goddard Institute for Space Studies, USA	2.5 × 2.0	085001-185012/ 185101-200512
	IPSL-CM5A-LR	Institut Pierre Simon Laplace, France	3.8 × 1.9	085001-185012/ 185001-200512
	MIROC-ESM	Japan Agency for Marine-Earth Science and Technology, Atmosphere and Ocean Research Institute (The Univ. of Tokyo), and National Institute for Environmental Studies	2.8 × 2.8	085001-184912/ 185001-200512
	MPI-ESM-P & MPI-ESM-LR†	Max Planck Institute for Meteorology, Germany	1.88 × 1.87	085001-184912/ 185001-200512
	MRI-CGCM3	Meteorological Research Institute, Japan	1.1 × 1.1	085001-185012/ 185001-200512

† MPI-ESM-P was used to obtain projections for the past 1000 (850-1850 CE) and historical experiments (1850-2000 CE). The MPI-ESM-LR GCM was used for future projections (e.g., RCP 8.5, 2006-2100).

Table D2. Performance metrics to evaluate GCM skill in Alaska from 1951-2000.
V: Climate variable (P = Total annual precipitation, T = Mean July temperature).

Performance metric	Description
SpaceCor. – *V*	Spatial correlation between observed and GCM climatological normals (1950-2000)
RMSE – *V*	Root Mean Squared Error of monthly climate averages (Eq. 1)
Trend – *V*	Annual trend (1951-2000)
TimeVar.01yr. – *V*	Annual temporal variability (*SD* for T; *CV* for P)
TimeVar.10yr. – *V*	Decadal temporal variability (*SD* for T; *CV* for P)

Table D3. Summary of total relative errors for each GCM and observational dataset. Mean and SD indicate total relative error averages and standard deviations among all three observational datasets for each GCM.

		Observed				
		CRUTS323	UDelaware	ERA20C	**Mean**	**SD**
GCM	GISS-E2-R	2.97	4.05	2.69	3.24	0.71
	IPSL-CM5A-LR	6.09	5.95	4.96	5.67	0.62
	MIROC-ESM	7.27	7.18	6.10	6.85	0.65
	MPI-ESM-P	3.12	2.92	5.34	3.79	1.34
	MRI-CGCM3	4.53	4.92	3.69	4.38	0.63

Appendix E: *Bias-correcting and downscaling GCM data in Alaska*

To resolve spatial resolution differences between our statistical models (2 km) and GCM (> 1.0° Lat. × Lon.), we conducted a bias correction and spatial downscaling analysis. This technique downscaled GCM estimates to 2-km resolution, specifically using the delta-change method (Giorgi & Mearns 1991). Specifically, this methods uses bilinear interpolation on GCM grid cell anomalies (differences for temperature, ratios for precipitation) between monthly GCM output and historical 30-yr monthly climatologies from 1961-1990 to 2-km resolution. These interpolated anomalies for temperature (precipitation) are then added (multiplied) to gridded 2-km observational climate normals for 1961-1990. Here, we use the Parameter-elevation Regressions on Independent Slopes Model (PRISM) as our observational dataset in the downscaling process (Daly *et al.* 2008; PRISM Climate Group, Oregon State University, http://prism.oregonstate.edu, accessed September 4, 2011). We chose to use this downscaling method and observational dataset as they are identical to methods used by the Scenarios Network for Alaska and Arctic Planning (2015a,b), and thus also used in Young *et al.* (2017).

Appendix F: *Metadata and additional details for Alaskan paleo-fire-history records*

Table F1. Details for each of the 29 paleo-fire-history reconstructions used for model validation.

Site name	Lat., Lon. (decimal deg.)	Ecoregion	Oldest fire in analysis (yr CE)	Fire freq. 850-1850 CE (#/1000 yr)	Source
Chopper	66.00N, 156.28W	Yukon Flats	958	9	Kelly *et al.* 2013
Epilobium	65.97N, 145.57W	Yukon Flats	1039	6	Kelly *et al.* 2013
Granger	66.06N, 145.65W	Yukon Flats	878	13	Kelly *et al.* 2013
Jonah	66.07N, 145.09W	Yukon Flats	868	15	Kelly *et al.* 2013
Landing	65.90N, 145.78W	Yukon Flats	1048	4	Kelly *et al.* 2013
Latitude	65.93N, 146.14W	Yukon Flats	968	11	Kelly *et al.* 2013
Lucky	66.02N, 145.53W	Yukon Flats	998	9	Kelly *et al.* 2013
Noir	66.00N, 145.93W	Yukon Flats	1018	5	Kelly *et al.* 2013
Picea	65.88N, 145.59W	Yukon Flats	858	8	Kelly *et al.* 2013
Reunion	66.02N, 146.12W	Yukon Flats	879	8	Kelly *et al.* 2013
Robinson	65.97N, 145.70W	Yukon Flats	859	9	Kelly *et al.* 2013
Screaming Lynx	66.07N, 145.40W	Yukon Flats	1377	7	Kelly *et al.* 2013
West Crazy	65.89N, 145.62W	Yukon Flats	1127	7	Kelly *et al.* 2013
Windy	66.04N, 145.76W	Yukon Flats	868	6	Kelly *et al.* 2013
Crater	62.10N, 146.24W	Copper River Basin	1331	3	Barrett *et al.* 2013
Hudson	61.88N, 145.67W	Copper River Basin	986	3	Barrett *et al.* 2013
Minnesota Plateau	62.54N, 146.24W	Copper River Basin	881	6	Barrett *et al.* 2013
Super Cub	62.30N, 145.35W	Copper River Basin	896	3	Barrett *et al.* 2013
Code	67.16N, 151.86W	Kobuk Valley	936	7	Higuera *et al.* 2009
Ruppert	67.07N, 154.25W	Kobuk Valley	967	4	Higuera *et al.* 2009
Wild Tussock	67.13N, 151.38W	Kobuk Valley	937	6	Higuera *et al.* 2009
Little Isac	67.94N, 160.80W	Noatak	912	3	Higuera *et al.* 2011
Poktovik	68.03N, 161.38W	Noatak	897	5	Higuera *et al.* 2011
Raven	68.01N, 162.04W	Noatak	957	5	Higuera *et al.* 2011
Uchugrak	68.05N, 161.73W	Noatak	987	7	Higuera *et al.* 2011
Keche	68.02N, 146.92W	Brooks Range	1068	1	Chipman *et al.* 2015
Perch	68.94N, 150.50W	Brooks Foothills	-4586	0	Hu *et al.* 2010, Chipman *et al.* 2015
Upper Capsule	68.63N, 149.41W	Brooks Foothills	-4550	0	Chipman *et al.* 2015
Tungak	61.43N, 164.20W	Yukon-Kusk. Delta	-5019	0	Chipman *et al.* 2015

Appendix G: *Modifying the shape of fire-temperature relationships*

To modify the shape of the original fire-temperature relationship in Alaska (Figure 2c), we artificially increased the number of fire occurrences over a pre-specified temperature range. Specifically, our goal was to incrementally linearize this relationship, so we chose a temperature range that spanned the threshold response at 13.4 °C, here 7-15 °C. Across this range, we selected all available observations where fire had not occurred (i.e., fire absence), and then randomly selected a given number of these absences and "switched" them to fire occurrences. The number of switches was done at three different levels to proportionally increase the total number of fire occurrences in Alaska by 5%, 10%, and 25%. Across the 7-15 °C temperature range, the number of absences switched to occurrences was not uniformly distributed, but rather weighted to switch more observations under warmer temperatures and less under cooler temperatures. This weighting was accomplished by employing a Beta probability density function. We set Beta parameters to $\alpha = 3$ and $\beta = 1$, and under this setting we rescaled Beta quantiles (naturally spanning 0-to-1) to the scale of the temperature range (7-15 °C). Under this rescaling, probability density values were associated with a given temperature and used as the weights for random selection of fire absence. The three modified fire-temperature relationships created by increasing total fire occurrences in Alaska by 5%, 10%, and 25% are designated by S1-S3 (Figure G1).

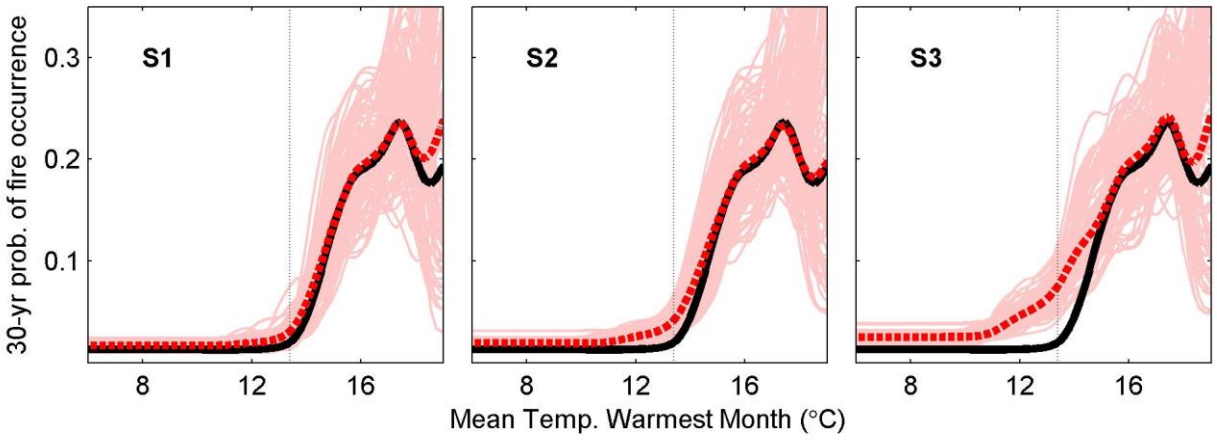

Figure G1. Three modified relationships (S1-S3) used in the sensitivity analysis. The black line is the median prediction of the 100 BRTs from the original relationship (i.e., unmodified). The dashed red line is the median prediction for the modified relationship, and the light pink lines are the predictions for individual, modified BRTs. The vertical line indicates the estimated threshold value under the original fire-temperature relationship (i.e., 13.4 °C).

Appendix H: *Projected future temperatures by Alaskan ecoregion (RCP 6.0)*

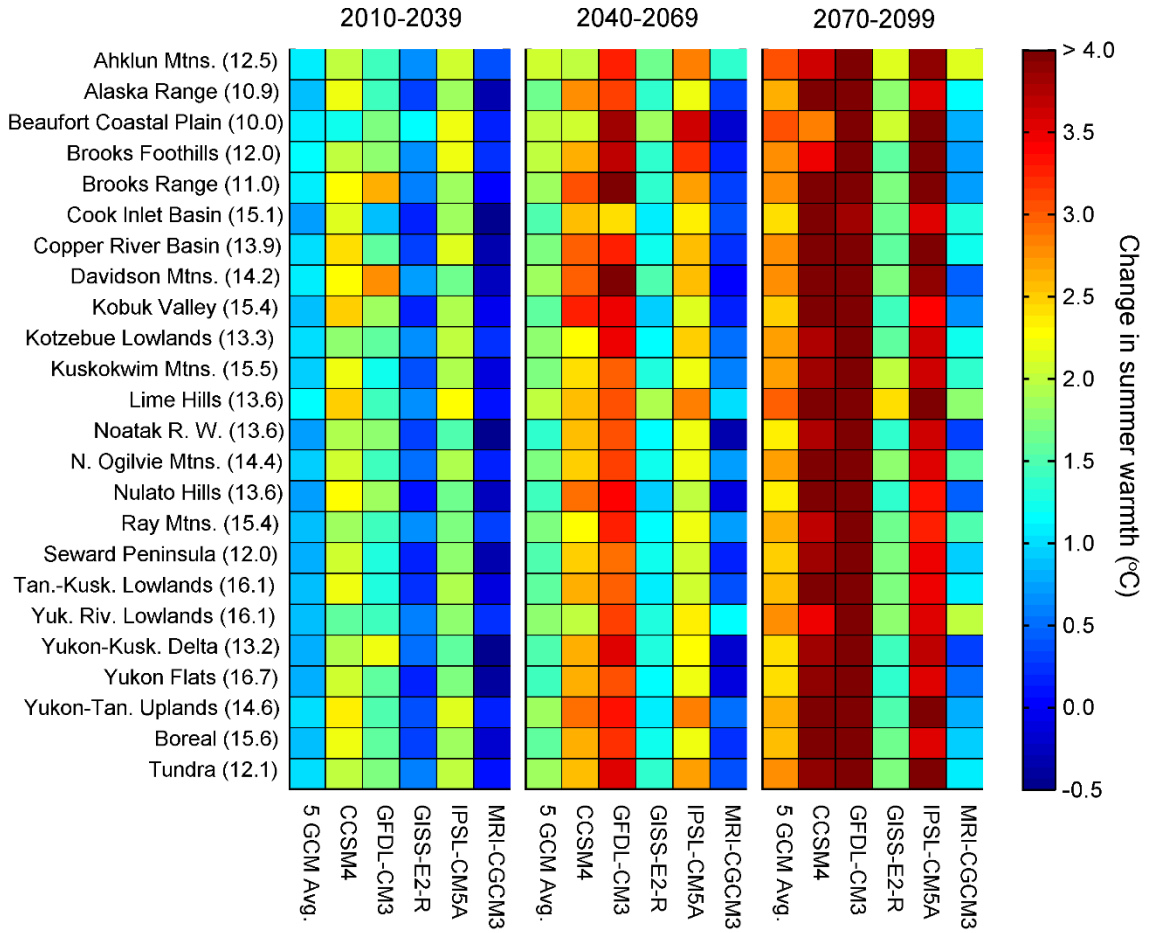

Figure H1. Projected changes in summer warmth (i.e., mean temperature of the warmest month) for Alaskan ecoregions and the boreal forest and tundra spatial domains. Values in parentheses next to ecoregion names are the 1950-2009 averages, while colors indicate the magnitude of projected change for the five-GCM average and each GCM individually. Projected changes were calculated by taking the difference in projected climate for each 2-km pixel and then averaging this difference across each region and time period. Projections were provided by the Scenarios Network for Alaska and Arctic Planning (2015b). This figure was first published in Young *et al.* (2017) as Figure A5.

Appendix I: *Comparing GCM and paleo-proxy temperatures, 850-2000 CE*

To identify potential biases in past-millennium GCM projections, we compared our downscaled GCM temperature estimates for 850-2005 CE (Appendix E) with paleo-climate reconstructions. To conduct these comparisons, we selected seven paleo-temperature reconstructions from Alaska (Table I1), bias-correcting each of these records relative to downscaled CRU Time Series temperature data for 1901-2005 (Harris *et al.* 2014; Scenarios Network for Alaska and Arctic Planning 2015a). Specifically, we added the average temperature difference between observed and proxy temperatures for 1901-2005 CE to the original paleo-temperature estimates. Additionally, for midge-based temperature reconstructions (Table I1), we linearly interpolated temperature estimates between individual samples in the paleo-record to an annual timescale. Annual differences were subsequently taken between paleo-reconstructed and GCM-derived temperatures, and summarized for 850-2005 CE (Table I2). These GCM- and paleo-derived temperatures are further visualized in Figure I1.

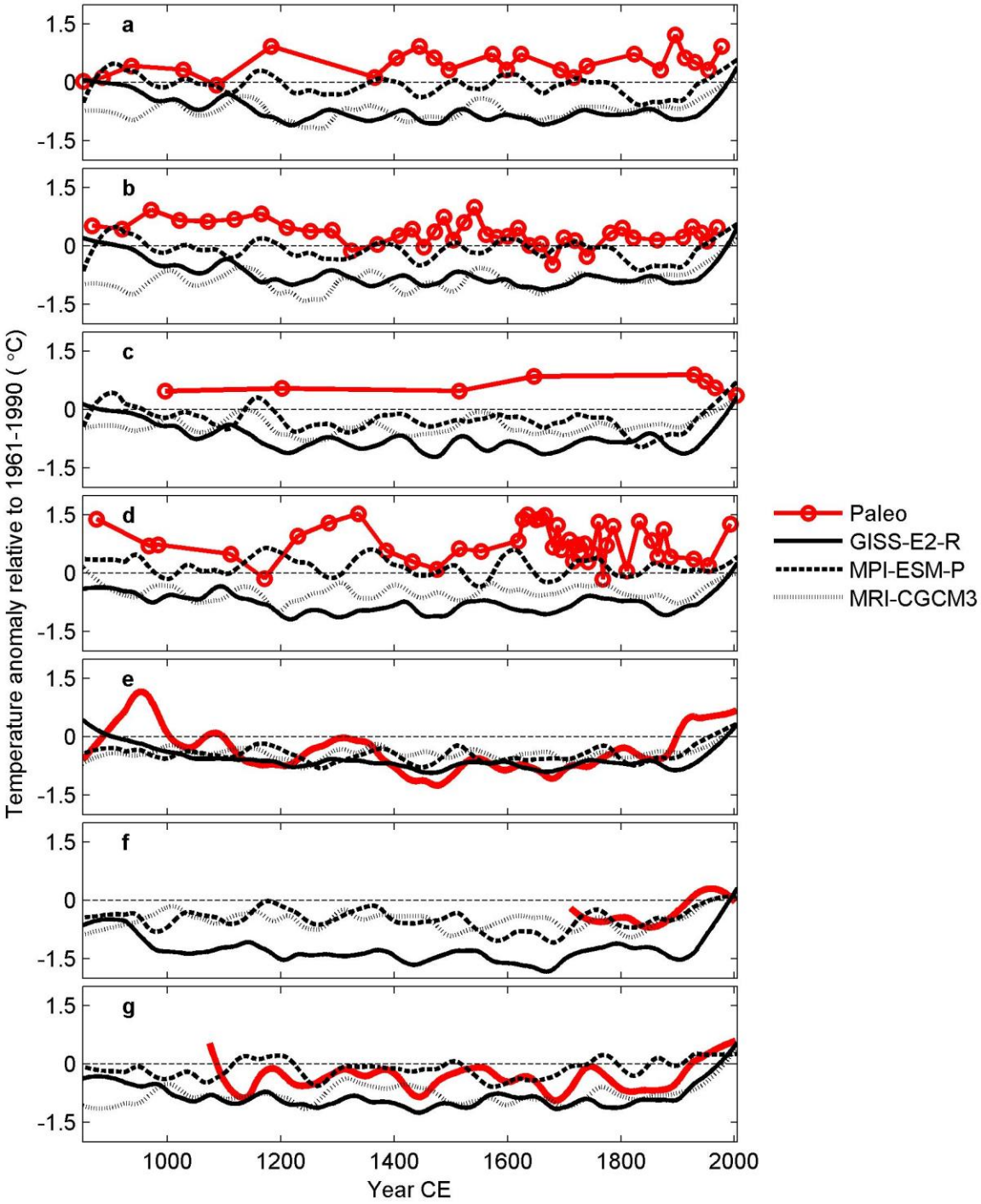

Figure I1. Time-series for paleo- and GCM-derived temperatures for (a) Hudson, (b) Moose, (c) Rainbow, (d) Screaming Lynx, (e) Gulf of Alaska, (f) Seward Peninsula, and (g) Firth River sites. GCM temperatures were smoothed using locally weighted regression (loess) with a span of 0.13 (≈150 yr), and tree-ring temperatures (e-g) were similarly smoothed. For chironmid-based reconstructions (a-d), the locations of individual samples in the records are indicated by open circles.

Table I1. Details for the seven paleo-proxy climate records used to assess GCM temperature biases from 850-2000 CE. All midge-based records were downloaded from the NOAA National Centers for Environmental Information (https://www.ncdc.noaa.gov/data-access/paleoclimatology-data). Tree-ring records were downloaded from the Northern Hemisphere Tree-Ring Network Development (N-TREND) consortium (Wilson *et al.* [2016]; https://ntrenddendro.wordpress.com/).

Site name	Lat., Lon. (decimal degrees)	Method	Time period covered	Source
Hudson	61.90N, 145.67W	Midge	7624 BCE to 1978 CE	Clegg *et al.* (2011)
Moose	61.37N, 143.60W	Midge	4508 BCE to 1970 CE	Clegg *et al.* (2010)
Rainbow	60.72N, 150.80W	Midge	11556 BCE to 2004 CE	Clegg *et al.* (2011)
Screaming Lynx	66.07N, 145.40W	Midge	8661 BCE to 1993 CE	Clegg *et al.* (2011)
Gulf of Alaska	Multiple locations[a]	Tree ring	800 to 2010 CE	Wiles *et al.* (2014)
Seward Peninsula	Multiple locations[b]	Tree ring	1710 to 2001 CE	D'Arrigo *et al.* (2004)
Firth River	68.39N, 141.38W	Tree ring	1073 to 2011 CE	Anchukaitis *et al.* (2013)

[a]Bounding box: NW corner = 61.11N, 149.00W, SE corner = 60.00N, 141.68W.
[b]Bounding box: NW corner = 65.22N, 162.27W, SE corner = 65.11N, 162.18W.

Table I2. Temperature differences between paleo- and GCM-derived temperatures (i.e., paleo minus GCM estimates) averaged over the time period of 850-2000 CE.

Site name	GCM	Paleo – GCM temperature differences Mean ± SD (°C)
Hudson	GISS-E2-R	1.20 ± 1.21
	MPI-ESM-P	0.55 ± 1.97
	MRI-CGCM3	1.21 ±1.36
Moose	GISS-E2-R	1.11 ± 1.22
	MPI-ESM-P	0.46 ± 2.00
	MRI-CGCM3	1.28 ± 1.53
Rainbow	GISS-E2-R	1.45 ± 1.19
	MPI-ESM-P	0.93 ± 2.00
	MRI-CGCM3	1.06 ± 1.15
Screaming Lynx	GISS-E2-R	1.51 ± 1.32
	MPI-ESM-P	0.56 ± 1.95
	MRI-CGCM3	1.22 ± 1.47
Gulf of Alaska	GISS-E2-R	0.23 ± 1.11
	MPI-ESM-P	0.10 ± 1.41
	MRI-CGCM3	0.08 ± 1.22
Seward Peninsula	GISS-E2-R	0.78 ± 1.44
	MPI-ESM-P	0.06 ± 1.66
	MRI-CGCM3	0.18 ± 1.36
Firth River	GISS-E2-R	0.54 ± 1.55
	MPI-ESM-P	-0.25 ± 1.59
	MRI-CGCM3	0.41 ± 1.60

Literature cited in appendices

Anchukaitis, K.J., D'Arrigo, R.D., Andreu-Hayles, L., Frank, D., Verstege, A., Curtis, A. *et al.* (2013). Tree-ring-reconstructed summer temperatures from northwestern North America during the last nine centuries. *J. Climate*, 26, 3001-3012.

Barrett, C.M., Kelly, R., Higuera, P.E. & Hu, F.S. (2013). Climatic and land cover influences on the spatiotemporal dynamics of Holocene boreal fire regimes. *Ecology*, 94, 389-402.

Chipman, M.L., Hudspith, V., Higuera, P.E., Duffy, P.A., Kelly, R., Oswald, W.W. *et al.* (2015). Spatiotemporal patterns of tundra fires: Late-Quaternary charcoal records from Alaska. *Biogeosciences*, 12, 4017-4027.

Clegg, B.F., Clarke, G.H., Chipman, M.L., Chou, M., Walker, I.R., Tinner, W. *et al.* (2010). Six millennia of summer temperature variation based on midge analysis of lake sediments from Alaska. *Quat. Sci. Rev.*, 29, 3308-3316.

Clegg, B.F., Kelly, R., Clarke, G.H., Walker, I.R. & Hu, F.S. (2011). Nonlinear response of summer temperature to Holocene insolation forcing in Alaska. *Proc. Natl. Acad. Sci. USA*, 108, 19299-19304.

D'Arrigo, R., Mashig, E., Frank, D., Jacoby, G. & Wilson, R. (2004). Reconstructed warm season temperatures for Nome, Seward Peninsula, Alaska. *Geophys. Res. Lett.*, 31.

Daly, C., Halbleib, M., Smith, J.I., Gibson, W.P., Doggett, M.K., Taylor, G.H. *et al.* (2008). Physiographically sensitive mapping of climatological temperature and precipitation across the conterminous United States. *Int. J. Climatol.*, 28, 2031-2064.

Giorgi, F. & Mearns, L.O. (1991). Approaches to the simulation of regional climate change - a review. *Rev. Geophys.*, 29, 191-216.

Harris, I., Jones, P.D., Osborn, T.J. & Lister, D.H. (2014). Updated high-resolution grids of monthly climatic observations - the CRU TS3.10 Dataset. *Int. J. Climatol.*, 34, 623-642.

Higuera, P.E., Brubaker, L.B., Anderson, P.M., Hu, F.S. & Brown, T.A. (2009). Vegetation mediated the impacts of postglacial climate change on fire regimes in the south-central Brooks Range, Alaska. *Ecol. Monogr.*, 79, 201-219.

Higuera, P.E., Chipman, M.L., Barnes, J.L., Urban, M.A. & Hu, F.S. (2011). Variability of tundra fire regimes in Arctic Alaska: millennial scale patterns and ecological implications. *Ecol. Appl.*, 21, 3211-3226.

Hu, F.S., Higuera, P.E., Walsh, J.E., Chapman, W.L., Duffy, P.A., Brubaker, L.B. *et al.* (2010). Tundra burning in Alaska: Linkages to climatic change and sea ice retreat. *J. Geophys. Res.-Biogeo.*, 115, G04002.

Kelly, R., Chipman, M.L., Higuera, P.E., Stefanova, I., Brubaker, L.B. & Hu, F.S. (2013). Recent burning of boreal forests exceeds fire regime limits of the past 10,000 years. *Proc. Natl. Acad. Sci. USA*, 110, 13055-13060.

Poli, P., Hersbach, H., Dee, D.P., Berrisford, P., Simmons, A.J., Vitart, F. *et al.* (2016). ERA-20C: an atmospheric reanalysis of the twentieth century. *J. Climate*, 29, 4083-4097.

Rupp, D.E., Abatzoglou, J.T., Hegewisch, K.C. & Mote, P.W. (2013). Evaluation of CMIP5 20th century climate simulations for the Pacific Northwest USA. *J. Geophys. Res.-Atmos.*, 118, 10884-10906.

Scenarios Network for Alaska and Arctic Planning, University of Alaska. 2015. Historical Monthly Temperature and Precipitation - 2 km CRU TS. Retrieved January 2015 from https://www.snap.uaf.edu/tools/data-downloads.

Scenarios Network for Alaska and Arctic Planning, University of Alaska. 2015. Projected Monthly Temperature and Precipitation - 2 km CMIP5/AR5. Retrieved January 2015 from https://www.snap.uaf.edu/tools/data-downloads.

Wiles, G.C., D'Arrigo, R.D., Barclay, D., Wilson, R.S., Jarvis, S.K., Vargo, L. *et al.* (2014). Surface air temperature variability reconstructed with tree rings for the Gulf of Alaska over the past 1200 years. *Holocene*, 24, 198-208.

Wilson, R., Anchukaitis, K., Briffa, K.R., Buntgen, U., Cook, E., D'Arrigo, R. *et al.* (2016). Last millennium northern hemisphere summer temperatures from tree rings: Part I: The long term context. *Quat. Sci. Rev.*, 134, 1-18.

Young, A.M., Higuera, P.E., Duffy, P.A. & Hu, F.S. (2017). Climatic thresholds shape northern high-latitude fire regimes and imply vulnerability to future change. *Ecography*, 40, 606-617.